Extracellular adenosine deamination primes tip organizer development in *Dictyostelium*

Pavani Hathi and Ramamurthy Baskar*

Bhupat and Jyoti Mehta School of Biosciences, Department of Biotechnology, Indian Institute of Technology-Madras, Chennai 600036, India.

*Correspondence: rbaskar@iitm.ac.in

Abstract

Ammonia is a morphogen in *Dictyostelium* and is known to arise from the catabolism of proteins and RNA. However, we show that extracellular adenosine deamination catalyzed by adenosine deaminase related growth factor (ADGF), is a major source of ammonia and demonstrate a direct role of ammonia in tip organizer development. The tip formed during early development in *Dictyostelium* is functionally similar to the embryonic organizer of higher vertebrates. *adgf* mutants fail to establish an organizer and this could be reversed by exposing the mutants to volatile ammonia. Interestingly, bacteria physically separated from the *adgf*$^{-}$ mounds in a partitioned dish also rescues the mound arrest phenotype suggesting a cross kingdom interaction driving development. Both the substrate, adenosine and the product, ammonia regulate *adgf* expression, and *adgf* acts downstream of the histidine kinase *dhkD* in regulating tip formation. Thus, the consecutive transformation of extracellular cAMP to adenosine, and adenosine to ammonia are integral steps during *Dictyostelium* development. Remarkably, in higher vertebrates, *adgf* expression is elevated during gastrulation and thus adenosine deamination may be an evolutionarily conserved process driving organizer development.

Key words

adenosine deaminase, organizer development, tip formation, volatile ammonia, *Dictyostelium*

Introduction

During early embryonic development, organizers play an important role in patterning and directing the differentiation of surrounding cells into specific tissues and organs. The embryonic organizer establishes the developmental polarity in vertebrates and similarly, the mound/slug tip in *Dictyostelium* act as organizers (Rubin and Robertson, 1975) playing a pivotal role in guiding collective cell migration and patterning. Despite numerous investigations on *Dictyostelium* tip formation, the processes by which the tip establishes and maintains the primary developmental axis remains elusive. Gaining insights into the mechanisms regulating tip organizer function will offer a valuable understanding of the orchestrated cell movements and intricate processes underlying development.

Study of the social amoeba *Dictyostelium discoideum* has helped us to better understand many fundamental problems about development (Annesley and Fisher, 2009; Müller-Taubenberger et al., 2013; Dunn et al., 2018; Martín-González et al., 2021; Huber et al., 2022). *Dictyostelium* has demonstrated its value in a range of applications, including the investigation of human diseases (Eichinger et al., 2005; Müller-Taubenberger et al., 2013; Storey et al., 2022). *Dictyostelium* are free living, amoeboid, soil protists and alternate their life cycle between unicellular and multi-cellular stages. The amoebae prey on bacteria and upon starvation, the cells aggregate gradually forming a tipped multicellular mound. The mound further develops to form a slug which undergoes differentiation and morphogenesis to form a fruiting body consisting of a dead stalk supporting a ball of spores (Raper, 1940; Kessin, 2001).

44 Diffusible molecules such as cAMP, adenosine, ammonia, and a chlorinated hexaphenone
45 'differentiation-inducing factor' (DIF) regulate multicellular development in *Dictyostelium*
46 (Bloom and Kay, 1988; Williams, 1988; Gross, 1994; Mahadeo and Parent, 2006; Shu et al.,
47 2006). The gradient of these morphogens along the slug axis determines the cell fate, either as
48 prestalk (pst) or as prespore (psp) cells. cAMP regulates PKA activity, adenosine signaling, and
49 morphogenetic cell movements to control tip development in *Dictyostelium* (Mann and Firtel,
50 1993; Siegert and Weijer, 1995). Adenosine, a by-product of cAMP hydrolysis, acts as an
51 inhibitory morphogen suppressing additional tip formation (Schaap and Wang, 1986), however
52 the mechanism involved in tip formation is not completely understood.

53 Adenosine deaminase (ADA) or its isoforms regulate adenosine homeostasis by catalysing the
54 breakdown of adenosine to generate inosine and ammonia, and are conserved among bacteria,
55 invertebrates, vertebrates including mammals (Cristalli et al., 2001). Two isoforms of ADA are
56 known in humans including ADA1 and ADA2 and ADGF shares a structural similarity to ADA2.
57 ADA2 is associated with the activation of lymphocytes that play a role in the immune response
58 to infections (Marone et al., 1980). Absence of ADA2 activity results in the build-up of
59 deoxyadenosine and its phosphorylated metabolite, dATP that is toxic to lymphoid precursors
60 (Notarangelo, 2016). Consequently, complete ADA2 deficiency is characterized by lymphopenia
61 and severe combined immuno-deficiency disorder (SCID) (Gaspar, 2010). The loss-of-function
62 mutations in *adgf/ada2* in humans also manifest in a variety of vascular and inflammatory
63 symptoms, including early-onset of stroke and systemic vasculopathy (Zhou et al., 2014).

64 *ada2* disruption in mice leads to liver dysfunction and perinatal mortality (Wakamiya et al., 1995)
65 and transgenic overexpression of ADA2 in mice results in aberrant heart and kidney
66 development (Riazi et al., 2005). Absence of *adgf/ada2* in frogs manifests in reduced body size

67 with altered polarity (Iijima et al., 2008). In *Drosophila*, six ADGFs have been identified and are
68 reported to promote cell proliferation by depleting extracellular adenosine (Zurovec et al., 2002).
69 Loss of function of *adgfA* in *Drosophila* promotes melanotic tumour formation and larval death
70 (Dolezal et al., 2005). In *Arabidopsis thaliana*, tRNA adenosine deaminase 3 (*tad3*) is necessary
71 for telomere length homeostasis (Bose et al., 2020). Adenosine deaminases are known to interact
72 with dipeptidyl peptidase IV (DPP), CD26 (cluster of differentiation 26) expressed on T-cells
73 and the adenosine receptor, A2AR (expressed on dendritic cells) to facilitate cell-cell signaling
74 (Moreno et al., 2018). Thus, *adgf* plays a pivotal role in the regulation of cell proliferation and
75 development in several organisms.

76 Four isoforms of ADA are annotated in the *Dictyostelium discoideum* genome (Eichinger et al.,
77 2005) including adenosine deaminase (*ada*; DDB_G0287371), adenosine deaminase acting on
78 tRNA-1 (DDB_G0278943), adenosine deaminase tRNA-specific (DDB_G0288099) and
79 adenosine deaminase-related growth factor (*adgf*; DDB_G0275179), and their role in growth and
80 development is not known. In this study, we examined the role of *adgf* during multicellular
81 development in *D. discoideum* and demonstrate that ammonia derived from adenosine
82 deamination is directly involved in tip organizer development.

83 **Results**

84 **Differential regulation of *adgf* expression during growth and development**

85 To verify the blasticidin *(bsr)* insertion in *adgf* $^{-}$, a diagnostic PCR was carried out and the
86 integration was validated (Figures 1A and 1B), and qRT-PCR analysis confirmed the absence of
87 *adgf* expression (Figure 1C). In vertebrates, adenosine deaminases are expressed in a tissue
88 specific manner to control growth and development. To know if *adgf* expression is differentially

89 regulated during development in *Dictyostelium*, qRT-PCR was performed using RNA obtained
90 from different stages of development. The time point of analysis includes 0 h, 8 h, 12 h, 16 h, 20
91 h and 24 h. *adgf* expression peaks at 16 h (Figure 1D) implying an important role for *adgf* later in
92 development. At this time point, the expression of the other three isoforms of ADA were not
93 significantly different from WT, suggesting that they do not compensate for the loss of *adgf*
94 (Figure 1E).

95 ***Dictyostelium* ADGF shares a strong structural similarity with human ADA2**

96 The *D. discoideum adgf* gene is predicted to encode a protein of 543 long amino acids and
97 belongs to the metallo-transferase superfamily (Figure 2A), containing a ADA domain and an N-
98 terminal domain similar to human ADA2 (Figure 2B). Using the ADGF sequence from the
99 protein family database (https://www.ebi.ac.uk/interpro/), an analysis was carried out using the
100 online tools, SMART (Simple Modular Architecture Research Tool: http://smart.embl-
101 heidelberg.de), to know the presence of structurally similar domains. This study suggests that the
102 protein domains of *Dictyostelium* ADGF are conserved and show high degree of similarity with
103 human *ada2*.

104 *D. discoideum* ADGF (DdADGF) shares 37.47% identity with human ADA2. ADGF is present
105 in other social amoeba, sharing a sequence similarity of 59.5% with *Dictyostelium fasciculatum*,
106 61.2% with *Dictyostelium pupureum,* 53.6% with *Dictyostelium lacteum* and 62.1% with
107 *Polysphondylium pallidum* (www.uniprot.org). Multiple sequence alignment reveals the presence
108 of an N-terminal signal sequence characteristic of extracellular proteins (Figure 2C) and
109 conserved histidine and glutamine residues in the active site of both *D. discoideum* ADGF and
110 human ADA2 (Figure 2D).

111 The phylogenetic relation of ADGF to the classic ADA subfamily has been reported previously
112 (Maier et al., 2005). To determine the evolutionary relationship of *D. discoideum* ADGF with
113 that of other organisms, a phylogenetic analysis was carried out and the alignment was created
114 using MEGAX software (Kumar et al., 2018). The evolutionary history of ADGF was inferred
115 using a Maximum Likelihood approach with Bootstrap analysis (100 iterations) as described by
116 Felsenstein (1985). The resulting phylogenetic tree indicated that DdADGF is closely related to
117 the ADGF proteins of other Dictyostelid members, including D. purpureum, Heterostelium
118 pallidum, and Cavenderia fasciculata. *D. discoideum* ADGF forms a distinct clade, likely
119 representing a distant relative of its vertebrate homolog (Figure 2E). Additionally, the structure
120 of *D. discoideum* ADGF was predicted by homology modeling with AlphaFold
121 (https://alphafold.ebi.ac.uk/), using the crystal structure of human ADA2, CECR1 (Cat eye
122 syndrome critical region protein 1) as a template (PDB-3LGD) (Figures 2F-H). Alignment of
123 *Dictyostelium* ADGF with human ADA2 yielded an RMSD value of 1.003 Å, indicating strong
124 structural similarity (Eidhammer et al., 2000; Koehl, 2001).

125 ***adgf* controls aggregate size in *Dictyostelium***

126 To understand the role of *adgf* during *D. discoideum* development, mutant lines with lesions in
127 the gene *adgf* were plated at a density of $5x10^5$ cells/cm^2 on non-nutrient phosphate buffered agar
128 plates (pH 6.4) and monitored thereafter. In comparison to WT (37.6 ± 2.7 mm^2), the aggregates
129 of *adgf* $^-$ were larger in size (62.6 ± 5.4 mm^2; p value = 0.0003), and thus the number of
130 aggregates formed by the mutants were fewer (39.67 ± 3.703) than the WT (67.00 ± 2.543)
131 (Figure 3A). To determine the pathways that are affected impairing the tissue size in the mutant,
132 RNA expression of countin (*ctn*) and small aggregates (*smlA*) were examined and their levels
133 were found to be reduced significantly compared to controls (Figure 3B). Countin factor (CF)

134 regulates group size by reducing the expression of cell-cell adhesion proteins cadherin (*cadA*)
135 and contact site A (*csaA*) (Siu et al., 1985). The expression of *cadA, csaA* and cell-cell adhesion
136 were also quantified and the mutants displayed enhanced *cadA* and *csaA* expression and higher
137 cell-to-cell contacts than the WT (Figures 3C and 3D) suggesting that *adgf* regulates the overall
138 size of the aggregates.

139 cAMP chemotaxis significantly influences cell-cell adhesion (Konijn et al., 1967) and to know if
140 chemotaxis is impaired in the mutant, an under-agarose chemotaxis assay was carried out. The
141 chemotactic activity was not significantly different between the two cell types (Figure 3E),
142 implying that the increased mound size in the mutant may not be due to altered chemotactic
143 activity.

144 ***adgf* mutants form large, tipless mounds**

145 Subsequent to plating on KK2 agar plates, WT cells formed mounds by 8-9 h, and culminate to
146 form fruiting bodies by the end of 24 h. In contrast, the *adgf* $^{-}$ lines were blocked as rotating
147 mounds with no tips till 30 h (Figure 3F; Supplementary videos S1 and S2). The mound arrest
148 phenotype could be mimicked by adding the ADA specific inhibitor deoxycoformycin (DCF) to
149 WT cells (Figure 3G). After 36 h, a fraction of *adgf* $^{-}$ mounds (34.77 ± 4%) formed fruiting
150 bodies with bulkier spore sac and a stalk (Figures 3H and 3I). This late recovery from the mound
151 arrest may be due to the expression of other ADA isoforms after 36 h.

152 **Reduced ADA activity leads to high adenosine levels in the *adgf* mutant**

153 If the function of *adgf* is compromised, ADA enzyme activity is expected to be low. To verify
154 this, total ADA activity in WT and *adgf* $^{-}$ mounds was measured using a commercial kit. This
155 technique relies on the conversion of inosine (by ADA) to uric acid and was measured at

156 A293 nm. Although ADA activity was reduced significantly in the mutant (Figure 4A), it was
157 not completely abolished and possibly, other isoforms of ADA may have a basal activity at 16 h.

158 ADGF quenches extracellular adenosine and if this process is impaired as expected in *adgf*$^{-}$, the
159 mutants will have increased extracellular adenosine. Using a commercial kit, total adenosine
160 levels were measured and the adenosine levels were elevated both at 12 h and 16 h in the mutant,
161 (Figure 4B) and this difference was highly significant at 16 h (377.6 ± 18.86 nM in the WT;
162 490.8 ± 7.241 nM in the mutant, $p = 0.0002$). *adgf* expression, at this time point was also high in
163 WT cells. The elevated adenosine levels at 16 h may be due to reduced ADA activity and
164 enhanced expression of genes such as 5' nucleotidase (*5'nt),* phosphodiesterases *(pdsA* and *regA)*
165 that are involved in adenosine formation. Hence, their expression levels were examined.
166 Although the expression of both *5'nt* and *regA* were enhanced at 8 h, *pdsA* levels remain
167 unaltered. Interestingly, the expression of all three genes trended lower at 12 h but were
168 significantly upregulated at 16 h (Figure 4C) suggesting an important role of these genes at a
169 specific time in development.

170 **Addition of ADA or overexpression of *adgf* cDNA restored tip development in *adgf*$^{-}$**

171 *adgf* mutants carry significantly high levels of adenosine. By administering ADA enzyme on top
172 of the *adgf*$^{-}$ mounds (Figure 5A), excess adenosine can be quenched resulting in ammonia
173 formation, possibly rescuing the phenotype. Indeed, addition of 10 U ADA onto mutant mounds
174 restored tip development. Besides, overexpression of WT *adgf* cDNA (driven by actin15
175 promoter) rescues the developmental defects of the *adgf* mutants (Figures 5B and 5C),
176 confirming that the developmental block is the result of *adgf* gene disruption alone. However,
177 *adgf* cDNA overexpression in WT cells does not result in any observable defects (Figure 5D).
178 Taken together, these findings support an important function of *adgf* in tip development.

179 **WT or its conditioned media (CM) restored tip formation in *adgf*⁻ mounds**

180 In order to determine whether *adgf* is necessary for tip formation in a cell-autonomous manner,
181 WT and the mutant cells were reconstituted in different proportions and plated. In a mix of 50%
182 WT: 50% mutant, WT cells were able to rescue the defects of *adgf*⁻ cells but with 20% WT and
183 80% *adgf*⁻, the rescue was partial (31 ± 4 %) (Figure 5E) suggesting that the mound arrest
184 phenotype of the mutant is due to the absence of some secreted factor(s).

185 Further, when developed in the presence of WT CM, *adgf*⁻ cells formed tipped mounds and
186 eventually fruiting bodies (Figure 5F). Conversely, in the presence of CM from *adgf*⁻ cells, WT
187 developed as large mounds with no tips (Figure 5G) and the size was comparable to the mounds
188 formed by *adgf*⁻. These findings imply that the developmental phenotype of *adgf*⁻ is not due to a
189 cell autonomous defect but due to faulty secreted factor signaling.

190 **Volatile ammonia rescued the mound arrest phenotype of *adgf*⁻**

191 If ADGF function is compromised, ammonia levels are expected to be low. Hence, the
192 concentration of ammonia from WT and *adgf*⁻ mounds were measured using a commercial kit.
193 At the mound stage, total ammonia levels were significantly reduced in *adgf*⁻ lines (Figure 6A).
194 By mixing sodium hydroxide and ammonium chloride (Thadani et al., 1977), ammonia could be
195 generated, and in such conditions, tip formation was restored in *adgf*⁻ mounds (Figure 6B).

196 **Physically separated WT restored tip development in the mutant**

197 WT mounds are expected to release lot of volatiles including ammonia, possibly rescuing the
198 mound arrest phenotype of the mutants nearby. To verify if this is correct, *adgf*⁻ cells were
199 developed in one half of a compartmentalized Petri dish and WT cells on the other side.
200 Interestingly, the mound arrest of *adgf*⁻ was completely rescued by 3.5 hours (Figure 6C) in the

201 presence of WT although they were physically separated from each other. This suggests that
202 volatiles, likely to be ammonia released from WT is sufficient enough to rescue the mutant
203 phenotype.

204 The CM from *adgf*$^{-}$ is expected to have high adenosine, possibly generating low or no ammonia.
205 Addition of ADA to the CM of the mutant in one compartment of the partitioned dish led to a
206 partial rescue (57 % ± 2) of *adgf*$^{-}$ kept on the other side of the dish after 3.5 h (Figure 6D)
207 implying that the ammonia generated in such conditions may not be enough for a full rescue.

208 **Adenosine deamination alone drives the rescue of *adgf*$^{-}$**

209 To know if adenosine deamination is exclusively responsible for the rescue of the mutant, 10 ml
210 cold KK2 buffer mixed with different concentrations of adenosine (10 µM, 0.1 mM, 1 mM) was
211 added on one side of the compartmentalized dish and the other side of the dish had the mutant on
212 phosphate buffered agar arrested at the mound stage. After 3.5 h of the addition of ADA enzyme
213 (10 U) to the buffered solution containing adenosine, a full rescue was observed (Figure 6E),
214 strongly indicating that volatile ammonia generated from adenosine deamination alone is
215 rescuing the defect. Ammonia is known to be produced during protein/RNA catabolism in
216 *Dictyostelium* (White and Sussman, 1961; Hames and Ashworth, 1974; Schindler and Sussman,
217 1977; Walsh and Wright, 1978) but the total protein and RNA levels were not significantly
218 different between WT and *adgf* mutants (Figure S1 A-B) suggesting that ammonia released from
219 adenosine deamination plays a crucial role in tip formation.

220 **Caffeine, not ammonia rescued the mound size of *adgf*$^{-}$**

221 Given that adenosine levels were elevated in the mutants, we attempted to rescue the large
222 mound size observed in the *adgf* mutants by treating them with the adenosine antagonist,

223 caffeine. Caffeine rescued this early developmental defect in a dose-dependent manner (Figure
224 6F). This suggests that *adgf* may be one of the regulators of group size in *Dictyostelium*. Since
225 the ammonia levels were lower in the mutant, we tested whether exposure to ammonia could
226 rescue the large aggregate size of the *adgf* mutant. Exposing the mutants to 0.01 M ammonia
227 soon after plating or six hours after plating, had no effect on the aggregate size of the mutants
228 (Figure 6G), suggesting that while some early effects may be mediated through adenosine
229 receptors, the later effects appear to be independent and likely influenced by ammonia.

230 **Faulty expression of cAMP relay genes in *adgf*$^-$**

231 cAMP signaling is crucial for tip development and determining cell fate in *Dictyostelium*
232 (Schaap and Wang, 1986; Saxe et al., 1993; Firtel, 1996; Singer et al., 2019). Hence, the
233 expression of genes involved in cAMP relay were measured in WT and *adgf*$^-$ cells by qRT-PCR.
234 Total cAMP levels and *acaA* gene expression were both low in the *adgf*$^-$ lines (Figures 7A and
235 7B). Treating the cells with the pkA activator 8-Br-cAMP or cyclic-di-GMP, the activator of
236 adenyl cyclase (Wang and Schaap, 1985; Chen and Schaap, 2012), reversed the *adgf*$^-$ mound
237 arrest phenotype (Figures 7C and D). Increasing the cyclic-di-GMP dose from 0.5 mM to 1 mM
238 resulted in the formation of multiple tips (Figure 7E). These observations further reinforce that
239 the mound arrest phenotype of the *adgf*$^-$ lines is due to faulty cAMP signaling. Blocking the
240 phosphodiesterase (*pde4*) activity could also lead to higher cAMP levels transiently. When
241 treated with 3-Isobutyl-1-methylxanthine (IBMX), a known PDE4 inhibitor (Bader et al., 2007;
242 Siegert and Weijer, 1989), there was no effect on tip formation in *adgf*$^-$ mounds (Figure 7F),
243 although caffeine restored tip formation (Figure 7G). Thus, in spite of impaired expression of
244 cAMP relay genes, the chemotaxis activity is not altered in the mutant.

245

246 **Circular instead of spiral cAMP waves in *adgf*⁻ mounds**

247 Low *acaA* expression, reduced cAMP levels and enhanced cell-cell contacts in *adgf*⁻ is likely to
248 impair cAMP wave propagation and to ascertain if this is true, the cAMP signal propagation in
249 WT and *adgf*⁻ mounds were compared using dark field optics. In contrast to the WT, which
250 displayed a spiral wave propagating center, the *adgf* mutant exhibited a circular wave
251 propagating center throughout, suggesting that the cAMP relay is impaired (Figure 7H;
252 Supplementary videos S3 and S4).

253 **Ammonia restores tip formation by regulating *acaA/pde4* expression**

254 *adgf* expression peaks at 16 h and to find if *adgf* expression is regulated by the substrate or the
255 product, WT cells treated with different concentrations of adenosine (100 nM, 1 μM, 0.5 mM),
256 were plated on KK2 agar plates and harvested at 16 h for RNA isolation. Independently, WT
257 mounds on KK2 agar plates were exposed to different concentrations of volatile ammonia (0.1
258 mM, 1 mM, 10 mM) for 3 h and thereafter, the mRNA expression levels of *adgf*, *acaA* and *pde4*
259 were examined. All the rescue experiments involving ammonia is for 3.5 h time period. With 100
260 nM adenosine, the expression of both *adgf* and *acaA* decreased when compared to controls but at
261 higher adenosine concentrations (1 μM, 0.5 mM), the expression levels of these two genes were
262 comparable to controls (Figure 8A). Interestingly, *pde4* expression decreased gradually with
263 increasing adenosine concentrations (100 nM to 0.5 mM), but increased steadily with increasing
264 ammonia levels.

265 In mounds exposed to 0.1 mM ammonia, the expression of *adgf* decreased but exposure to 1 mM,
266 and 10 mM ammonia, respectively caused a 3 and 2.3-fold upregulation of *acaA* expression. This
267 observation suggests that ammonia may be rescuing the mound arrest phenotype by enhancing
268 *acaA* expression and thus cAMP levels. In similar conditions, a considerable increase in *pde4*

269 expression was observed (Figure 8B), which may be necessary for controlling cAMP production
270 in response to NH_3 treatment. In conclusion, the expression of *adgf* is influenced both by the
271 substrate adenosine as well as the product ammonia in a dose dependent manner.

272 **$adgf^-$ cells sort to prestalk in a chimera with WT**

273 To determine if *adgf* favours the differentiation of one cell type over the other, the expression of
274 prestalk (pst) and prespore (psp) markers were examined in the mutant by realtime PCR. While
275 the expression of pst markers, *ecmA* and *ecmB* were significantly upregulated, the psp-specific
276 *pspA* gene showed reduced expression in the mutant (Figure 8C), suggesting that WT *adgf*
277 favours psp expression.

278 To know the cell type preference of the *adgf* mutants in a chimera with WT, a fraction (20%) of
279 any one cell type was labelled with a cell tracker stain DIL and the development was tracked
280 thereafter. In the slugs that formed after reconstituting labelled WT or $adgf^{OE}$ cells with 80%
281 unlabelled $adgf^-$ cells, the fluorescence was largely confined in the psp region. Conversely,
282 when $adgf^-$ cells stained with DIL were reconstituted with unlabelled WT or $adgf^{OE}$, the
283 fluorescence was restricted to the pst part of the slug. In the reconstituted slugs, consistently,
284 labelled WT or $adgf^{OE}$ cells occupy the psp, whereas the $adgf^-$ cells end up in the pst region
285 (Figures 9A, 9B and 9C). Thus, the distribution of cell types in the mound/slug is significantly
286 influenced by *adgf,* as the mutant cells sort out in a mixture with WT cells and differentiate to pst
287 cells.

288 Further, when stained with the prestalk marker, neutral red (Yamamoto and Takeuchi, 1983), the
289 staining was intense in the pst and ALCs of $adgf^-$ slugs, and such an intense coloration was not
290 apparent in WT especially in the ALCs (Figure S2A). To further investigate if reduced ADA
291 activity affects cell type specific marker expression or their pattern in slugs, pst (*ecmA*-GFP,

292 *ecmO*-GFP) or psp (*pspA*-RFP) lines were treated with the ADA inhibitor DCF. While there was
293 no change in pst/psp patterns in the mounds and slugs that formed after a long delay, the *ecmA*-
294 GFP was intense in the tip when compared to WT (Figures S2B). Similar to NR staining pattern
295 in adgf mutant slugs, a prominent expression of *ecmA*-GFP was observed in the ALC region also.
296 Visually, there was no change in *ecmO* or *psp* marker expression in DCF treated slugs (Figures
297 S2C and S2D) suggesting that impaired ADGF activity affects tip specific expression
298 significantly.

299 ***adgf* acts downstream of the histidine kinase, *dhkD***

300 In an effort to identify the pathway by which *adgf* acts during tip development, we selected a
301 number of mutant lines with similar mound arrest phenotype such as cAMP receptor B (*carB* $^{-}$),
302 LIM domain containing protein (*limB* $^{-}$), mound mutants (*mndA* $^{-}$) and histidine kinase (*dhkD* $^{-}$)
303 (Saxe et al., 1993; Carrin et al., 1996; Chien et al. 2000; Singleton and Xiong, 2013) and treated
304 the mounds with ADA enzyme. Treatment with 10 U ADA or exposure to ammonia restored tip
305 formation in *dhkD* $^{-}$ mounds and not others tested (Figures S3A and S3C). An increase in ADA
306 concentration (20 U), resulted in the development of multiple tips in *dhkD*$^{-}$ (Figures 9D, 9E and
307 9F). These findings imply that *adgf* acts downstream of *dhkD* in controlling tip development.
308 Similarly, we tested few mutants with multiple tips phenotype, such as tipped mutant (*tipA* $^{-}$),
309 culinB (*culB* $^{-}$), autophagy mutants (*atg7* $^{-}$, *atg8*$^{-}$, and *atg9*$^{-}$) (Stege et al., 1999; Wang and Kuspa,
310 2002; Otto et al., 2003; Otto et al., 2004, Tung et al., 2010) by adding the ADA inhibitor, DCF (1
311 mM) to the cell suspension /agar plates and if rescued, those mutants are likely to be in the same
312 pathway controlling tip development. However, DCF treatment had no impact on mutants with
313 multiple tips (Figure S3B).

314

315 **Impaired expression of other deaminases also results in aberrant tip formation**

316 Several pathways control ammonia levels during development and knockouts in other
317 deaminases (2-aminomuconate deaminase: DDB_G0275081, adenosine monophosphate
318 deaminase: DDB_G0292266, dCTP deaminase: DDB_G0293580, threonine deaminase:
319 DDB_G0277245, N-acetyl glucosamine deaminase: DDB_G0286195, glucosamine-6-phosphate
320 deaminase: DDB_G0278873) show a partial mound arrest phenotype (Figures S4A-F) although
321 the expression of some of these candidates is stronger during development suggesting a
322 prominent and unique role of adenosine deamination in tip development.

323 **High adenosine levels and other related purines do not block tip development**

324 ADA catalyses the conversion of adenosine/deoxy adenosine respectively to inosine/ deoxy
325 inosine. As *adgf* mutants have high adenosine levels, we investigated if the mound arrest could
326 be mimicked in WT by treating with adenosine. Surprisingly, addition of adenosine does not lead
327 to mound arrest in WT (Figure S5A). It is possible that ADA/ADGF converted adenosine
328 analogues to inosine analogues, which in some manner affected development. Hence, WT cells
329 were treated with an adenosine analogue (2'-deoxyadenosine), or guanosine (10 μM each) and
330 they do not cause a mound arrest phenotype either. Similarly, treating *adgf* $^{-}$ mounds with
331 inosine does not restore tip formation (Figures S5B and S5C) suggesting that the blocked tip
332 development is due to faulty adenosine deamination alone.

333 **Cross kingdom rescue of the *adgf* $^{-}$ mound arrest phenotype**

334 Just like WT *Dictyostelum* rescuing the mound arrest phenotype of the mutant, we examined if
335 bacteria physically separated from the mutants would rescue the phenotype. To check this,
336 *Klebsiella aerogenes* and *adgf* mutants were incubated adjacent to each other within a
337 compartmentalized KK2 agar plate. After 12 h, tip formation was restored in the mutants while

338 in the same time frame, the mounds in controls failed to form tips. Possibly, *Klebsiella* on KK2
339 with no nutrients would die releasing ammonia restoring tip development in *Dictyostelium*
340 (Figure S6).

341 **Discussion**

342 ***Dictyostelium* ADGF is likely to be secreted growth factor**

343 Multiple sequence alignments, experiments with conditioned media and cell type reconstitution
344 with WT suggests that ADGF is a secreted molecule. AMP deaminase, previously characterized
345 in the mollusk *Helix pomatia*, has been identified as a member of ADGF family (Tzertzinis et al.,
346 2023). It is important to note that ADGF is also known to act on 5′-adenosine monophosphate
347 (AMP) and deoxyadenosine. Studies on the characterization and expression of this growth factor
348 has shown that it is a secreted protein critical for embryonic and larval development in Pacific
349 abalone (Hanif et al., 2022), highlighting the broader role of ADGF in development across
350 species. The human ADA2 enzyme belongs to the novel family of ADGF and crystal structure of
351 ADA2 reveal the presence of a catalytic- and two unique ADA2-specific domains with novel
352 folds, responsible for protein dimerization and interaction with cell surface receptors.
353 Furthermore, the presence of a number of N-glycosylation sites, conserved disulfide bond, and a
354 signal peptide in ADA2 indicate that ADA2 is specifically adapted to function in the
355 extracellular environment (Zavialov et al., 2010).

356 **Possible reasons for increased mound size in the *adgf* mutant**

357 Enhanced cell adhesion influences cohesion and can impact the mound size (Roisin-Bouffay et
358 al., 2000). The cell-cell adhesion genes *cadA* and *csaA* (Coates and Harwood, 2001) were
359 upregulated in the mutant, leading to enhanced adhesion and larger mound size. While over-

360 secretion of *ctn* leads to stream breaking resulting in smaller aggregate formation (Brock and
361 Gomer, 1999), disruption of the *ctn* gene prevents this process, inducing large aggregate
362 formation. *ctn* in turn regulates *smlA* (Brock et al., 2003), impacting the overall aggregate size.
363 Thus, *adgf* mutants have reduced *ctn* and *smlA* expression manifesting large mound formation.
364 Indeed, cells treated with adenosine are known to form large aggregates (Schaap and Wang,
365 1986) and the first genetic evidence supporting the previous work is from *adgf* mutants, which
366 carry excess extracellular adenosine and form large aggregation streams.

367 **Pathways generating ammonia in *Dictyostelium***

368 Proteolysis during starvation is believed to be the main source of volatile ammonia in
369 *Dictyostelium* (Hames and Ashworth, 1974; Schindler and Sussman, 1977; White and Sussman,
370 1961), while RNA degradation is also attributed to yield ammonia during starvation (Walsh and
371 Wright, 1978). During development, amino acids, total protein and RNA levels are reported to
372 reduce with a significant increase in ammonia levels, thus equivocating the source of volatile
373 ammonia (Hames and Ashworth, 1974). Furthermore, several deaminases or enzymatic reactions
374 in *Dictyostelium* may also potentially generate ammonia (Supplementary Table S1). The
375 annotated *D. discoideum* genome contains five evolutionarily conserved family of ammonium
376 transporter/methylammonium permease/rhesus protein (Amt/Mep/Rh) encoding genes
377 (Eichinger et al., 2005), *amtA, amtB, amtC, rhgA,* and *rhgB,* which help in regulating ammonia
378 levels during growth and development. *amtA* and *amtC* antagonistically control developmental
379 processes and are involved in ammonium sensing or transport (Follstaedt et al., 2003; Kirsten et
380 al., 2005; Singleton et al., 2006).

381

382

383 **Role of ammonia during *Dictyostelium* development**

384 During early development in *Dictyostelium,* ammonia is known to inhibit aggregation (Schindler
385 and Sussman, 1979; Williams et al., 1984), affect aggregate territory size (Thadani et al., 1977),
386 aggregate density (Feit, 1988), cell fate (Gross et al., 1988), culmination (Davies et al., 1993),
387 and fruiting body size (Lonski, 1976). Ammonia is essential for differentiation in submerged
388 clumps (Sternfeld and David, 1979) and favours prolonged slug migration called 'slugging' over
389 culmination and influences psp over pst differentiation (Newell et al., 1969). Ammonia plays a
390 crucial role in orienting cell masses and accelerating the movement of aggregating cells (Bonner
391 et al., 1986). Enzymatic removal of ammonia causes the quick transition from slug to fruiting
392 thus controlling the morphogenetic pathways (Schindler and Sussman, 1977). By suppressing
393 DIF biosynthesis (Neave et al., 1983), ammonia favors psp over pst development in
394 *Dictyostelium* (Davies et al., 1993; Riley and Barclay, 1990). Further, ammonia prevents the
395 developmental transition of slugs to fruiting bodies (Bradbury and Gross, 1989; Wang and
396 Schaap, 1989). It is interesting to note that ammonia induces tip development (as in *adgf*
397 mutants), but subsequently, tips move away from a source of ammonia. Migration of slugs/
398 fruiting bodies away from ammonia, reflects a process by which fruiting bodies position
399 themselves from other structures to increase the possibility of spore dispersal (Kosugi and
400 Inouye, 1989). Ammonia by enhancing the collective movement of cells is believed to exert
401 negative chemotaxis (Bonner et al., 1986). Ammonia is known to inhibit tip formation in slugger
402 mutants, but in strains such as NC4 (Gee et al., 1994), ammonia exerts no effect on tip formation
403 as in AX4 (data not shown). The highly acidic, autophagic vesicles in pst cells (Gross, 2009) are
404 believed to catalyze the breakdown of proteins and RNA, also generating ammonia.

405 ADGF and its substrate, adenosine could serve as a localized source of ammonia. Indeed, cells
406 carrying high ATP, its derivatives cAMP (Bargoda et al., 2009; Singer et al., 2019) and
407 adenosine (Schaap and Wang, 1986), end up in the tip (Hiraoka et al., 2022). Further, 5'-
408 nucleotidase promoter activity is high in pstAB cells (Ubeidat et al., 2002) that significantly
409 covers the tip region suggesting high adenosine levels in the tip. However, extracellular 5'-AMP
410 can be derived from multiple sources such as hydrolysis of cAMP, ATP and RNA (Carpousis et
411 al., 1999).

412 As a gas, ammonia can diffuse generating a gradient; high in the slug front compared to the
413 posterior. Our results (Fig. 6A) also show that the amount of ammonia released from adenosine
414 is in the same order of magnitude as that from other sources (Yoshino et al., 2007). In *adgf*
415 mutants, ammonia levels may not be sufficient enough to neutralize the acidic vesicles and hence,
416 NR staining is intense in the pst region and the ALCs (Bonner, 1952). Thus, excess acidification
417 if not neutralized may lead to mound arrest and if ammonia acts on the acidic vesicles, then,
418 collective migration of cells leading to tip formation may be favoured.

419 Ammonia is crucial in regulating differentiation, metabolism, and gene expression (Liu et al.,
420 2022, Stein et al., 2013). Ammonium has been shown to induce aberrant blastocyst
421 differentiation, disrupt normal metabolic processes, alter pH regulation, and subsequently affect
422 fetal development in mice (Lane and Gardner, 2003). Newt *Triturus* exposed to ammonia show
423 dorsalization of the ventral marginal zone highlighting the capacity of ammonia to alter
424 embryonic axis formation (Yamada, 1950). Furthermore, research on avian embryos has revealed
425 significant ammonia content in developing eggs, suggesting a potential role for ammonia in the
426 energy metabolism during ontogenesis (Needham, 1926).

427

428 **Ammonia's effect on cAMP signaling in *Dictyostelium***

429 Ammonia is known to increase intracellular cAMP levels in *D. discoideum* (Riley and Barclay,
430 1990; Feit et al., 2001) but Schindler and Sussman, (1977) and Williams et al., (1984) reported
431 that high ammonia levels inhibit the synthesis and release of cAMP. However, some of these
432 experiments use ammonium carbonate (Schindler and Sussman, 1977), or ammonium chloride
433 (Williams et al., 1984), as a source of ammonia and the possibility of carbonate and chloride ions
434 interfering with development cannot be ruled out. In slugs, ammonia is shown to exert very little
435 effect on cAMP levels (Schaap et al., 1995). In *Dictyostelium mucoroides,* high ammonia levels
436 are known to block the production of extracellular cAMP. The effect of volatile ammonia on
437 aggregation seems to be species specific notably in *P. violaceum, P. pallidum, and D.*
438 *mucoroides* resulting in wider aggregation territories, while it was not observed in other species
439 such as *D. discoideum* and *D. purpureum* (Bonner and Hoffman, 1963).

440 Adenylate cyclase (AC) activity is regulated by various factors (Steer, 1975). At physiological
441 levels, ammonium ions increase AC activity in the rat brain by 40% (Yeung et al., 1989), but
442 lowered its activity in the liver by about 30% (Wiechetek et al., 1979). Ammonia has been
443 shown to increase the activity of AC-G in *Dictyostelium* sori (Cotter et al., 1999). High ammonia
444 levels by altering the pH, can affect the activity of numerous enzymes whose activity is pH
445 dependent and thus the activity of AC can be impacted by pH variations. *adgf* mutants with low
446 ammonia levels have reduced cAMP levels and a gradual increase in ammonia, cause a steady
447 but significant increase in *aca*A expression. In other systems (Rat brain), ammonia is known to
448 interact with manganese (Rivera-Mancía et al., 2012; Lu et al., 2020) and this divalent cation is
449 known to increase *aca*A expression in *Dictyostelium* (Loomis et al., 1979; Khachatrian et al.,
450 1987). Possibly, ammonia interacts with metal ions like manganese to form 'ammine complexes'

451 (Lipkowski and Galus, 1973), particularly in aqueous environments or under specific conditions
452 where the appropriate ligands are available and enhances cAMP levels thus rescuing the mound
453 defects of the mutant.
454 The decision between the formation of the tip (pst cells) and the ALCs are controlled by the tip's
455 production of ammonia, which prevents the migration of ALCs towards the tip (Sternfeld and
456 David, 1982; Feit et al., 1990). Consistent with this observation, our results show that *adgf*
457 mutant lines that have low ammonia levels exhibit enhanced *ecmA* and *ecmB* marker expression.
458 Mutants impaired in DIF-1 synthesis fail to develop pst-O cells in the slug and subsequently also
459 fail to form the basal disc in the fruiting body (Thompson and Kay, 2000). Similar to our
460 observations of cells with high adenosine occupying the tip of the slug, cells with high ATP (that
461 degrades to adenosine) levels, also end up in the centre of the tip (Hiraoka et al., 2022).

462 Tip organizer development in *Dictyostelium* depends on the differentiation and appropriate
463 sorting of pst and psp cells (Kay et al., 1978; Williams et al., 1989; Saxe et al., 1993; Williams,
464 2006), a process that relies on signaling of different morphogens including cAMP, adenosine,
465 DIF and ammonia (Bloom and Kay, Williams, 1988; 1988; Riley and Barclay, 1990; Gross et al.,
466 1994; 2006). These morphogens modify one another's effects, and determine the choice of the
467 differentiation pathway as well as the spatial arrangement of cells (Bloom and Kay, 1988). Thus,
468 the rescue of the *adgf* mutant upon exposure to ammonia is likely due to cAMP signaling and
469 cell-cell contact.

470 **Possible reasons for reduced cAMP levels in the *adgf* mutant**

471 The increased expression of PDE's (intra and extracellular) and reduced ACA expression could
472 well explain the lower cAMP levels in the mutant. ADA significantly regulates adenosine levels,
473 thus reducing the activation of adenosine-mediated receptors (Van Haastert, 1983). Two classes

474 of adenosine receptors including adenosine alpha- and beta-receptors are known to be expressed
475 in *Dictyostelium* (Theibert and Devreotes, 1984). When adenosine concentrations are high, beta-
476 receptors bound with adenosine inhibit the binding of cAMP to its receptors, thereby inhibiting
477 cAMP signaling (Newell, 1982; Van Haastert, 1983; Theibert and Devreotes, 1984). High
478 adenosine levels in the *adgf* mutant may also reduce cAMP levels via a similar mechanism.

479 *adgf* activity is likely to be different between pst and psp cells as reconstitution with different
480 cell types shows that cells with low adenosine and high ammonia levels end up in psp while cells
481 with excess adenosine and low ammonia attain pst cell fate. Cell death also results in
482 adenosine/ammonia formation and thus *adgf* activity is likely to be higher in pst than psp to
483 maintain low extracellular adenosine. The mound/slug tip is believed to carry high adenosine
484 levels restricting additional tip formation favouring lateral inhibition (Wang and Schaap, 1985)
485 and our results also show that *adgf*$^{-}$ cells with high adenosine goes to pst than the psp region.

486 **Distorted cAMP waves in mutant**

487 Collective cell movement within mounds is essential for cell sorting and the progression from
488 mounds to finger structures (Kellerman and McNally, 1999). In WT mounds, cAMP waves
489 propagate in a spiral pattern, while in mutants, waves propagate in a concentric circular pattern.
490 Initially, cAMP waves appear as concentric circles that, upon symmetry breaking, form spiral
491 waves (Siegert and Weijer, 1995). With successive wave propagation, the circular ring distorts,
492 and one end curls toward the pulsatile center, creating a spiral wave around the organizing center.
493 In *adgf* mutants, however, defective cAMP relay prevents this transition, likely due to lower
494 cAMP levels. A surge in phosphodiesterase inhibition is thought to regulate this shift from
495 concentric to spiral wave propagation (Palsson and Cox, 1996).

496 The mound/slug tip of *Dictyostelium* generates cAMP pulses (Traynor et al., 1992), and is
497 known to suppress additional tip formation (Farnsworth, 1973). Adenosine, that inhibits tip
498 formation represses *pde4* expression whereas ammonia, that promotes tip elongation, increases
499 *pde4* expression. Thus, the restoration of cAMP signaling and spiral wave propagation possibly
500 leads to the rescue of the *adgf* $^{-}$ mound arrest phenotype. Surprisingly adenosine exerts little
501 effect on tip development in WT cells and studies of Inouye (1989) also reinforce our
502 observations, showing that adenosine does not significantly influence the conversion of pst to
503 psp cells in shaking culture conditions.

504 **Adenosine deamination drives tip organizer development**

505 A crucial evidence supporting that adenosine deamination is singularly responsible for the rescue
506 of mound arrest comes from experiments where partitioned dish with buffered solution
507 containing adenosine on one side and the mutants on the other half of the dish. Addition of ADA
508 enzyme (10 U) to the buffered solution with adenosine fully restored the tipped mound formation
509 in the other half of the dish. Although ammonia's role in *Dictyostelium* development is well
510 established, this report is the first to show a novel role of ammonia in tip development. If natural
511 variants of *Dictyostelium* with no tips exist in soil, there is a likelihood that they will form
512 fruiting bodies when WT Dictyostelids are nearby. It is important to note that development of an
513 organism in its natural habitat is strongly influenced by volatiles nearby (Schulz-Bohm et al.,
514 2017).

515 **ADA in organizer development and gastrulation in vertebrates**

516 *ada/adgf* expression is found to be significantly high during gastrulation stages (Figure S7) in
517 several vertebrates (Pijuan-Sala et al., 2019; Tyser et al., 2021) and the process of gastrulation in
518 higher organisms and collective cell movement within the *Dictyostelium* mound are remarkably

519 similar (Weijer, 2009), suggesting an overlooked role of ammonia in organizer development. It is
520 likely that ADA plays a conserved, fundamental role in regulating morphogenesis in
521 *Dictyostelium* and other organisms including vertebrates. The human homologue of *adgf*,
522 CECR1, is a potential gene for the genetic disorder, Cat-eye syndrome and thus, *Dictyostelium*
523 may also serve as a model to study this condition.

524 **_dhkD_ functions upstream of _adgf_**

525 The histidine kinase *dhkD*, a member of the two-component family of histidine kinases, appears
526 to function upstream of *adgf*, adding to our understanding of the signaling cascade in
527 *Dictyostelium*. Histidine kinases play essential roles in regulating developmental transitions, with
528 *dhkC*, for example, initiating the late developmental program that ultimately leads to fruiting
529 body formation (Singleton et al., 1998). This function of *dhkC* is regulated in part by ammonia
530 levels, as low ammonia concentrations have been shown to inhibit the *dhkC* phospho-relay,
531 thereby influencing developmental outcomes (Kirsten et al., 2005). In *Dictyostelium*, several
532 histidine kinases, including *dhkA*, *dhkB*, *dhkC*, and *dokA*, coordinate cAMP signaling to
533 modulate the activity of PKA, a cAMP-dependent protein kinase that is essential for proper
534 development (Anjard and Loomis, 2003). These findings suggest the interdependencies within
535 the signaling network in regulating multicellular development in *Dictyostelium.*

536 **Model of ADGF action**

537 High extracellular cAMP at the slug front (Singer et al., 2019) is expected to generate high
538 adenosine, which however could arise from other sources and thus ammonia levels are expected
539 to be higher in the slug front compared to the back. Possibly, ammonia generated extracellularly
540 is quenched rapidly by the intracellular acidic compartments of pst cells, increasing its pH and
541 favouring collective cell movement driving mound/ slug tip development. It is important to note

542 that ammonia is known to promote psp than pst differentiation. Although ammonia is likely to be
543 formed from several sources in *Dictyostelium*, a critical threshold concentration of ammonia may
544 be necessary for tip development. The failure of even one pathway may result in a drop-in
545 ammonia levels, exerting an effect on development (Figure 10). Overexpression of *ecmA* and
546 downregulation of *pspA* (as measured by realtime PCR) in the mutant suggests that there is a
547 change in cell type differentiation as suggested by the sorting experiments. This could suggest
548 that the differentiation of the cells is blocked at an early prestalk cell fate. Thus, ammonia is
549 likely to be important for the maturation of tip cells.

550 Our study shows that *adgf* acts downstream of *dhkD* and *in silico* studies have shown that *dhkD*
551 interacts with *adgf* (Figure S8A). Therefore, it is likely that in the presence of ammonia, *dhkD*
552 activates the phosphorelay, in turn increasing intracellular cAMP levels, leading to tip formation.
553 Histidine kinase *dhkC* is known to phosphorylate *regA* in *Dictyostelium* (Thomason et al.,1999).
554 However, based on docking we found no direct interaction of *regA* with ADGF (data not shown).
555 Thus, the integration of cytokinin and histidine kinase signaling ensures coordinated
556 multicellular organization in *Dictyostelium* (Aoki et al., 2020). Previous work in other systems
557 have found ADA to be interacting with CD 26 (dpp IV) (Tanaka, 1993) and docking DdADGF
558 with AprA (dpp8) (Figure S8B) also support the observations. However, adding ADA inhibitor
559 to *aprA* mutant (dpp8), show no effect on the phenotype (data not shown).

560 Organisms from different kingdoms often interact in complex ways such as symbiosis, predation,
561 competition etc., which can have significant effects on ecosystem dynamics (Helgason et al.,
562 1998; Harrison, 2005). Such interactions are often mediated through volatiles affecting the
563 physiology of each other just like the bacterial volatiles affecting the development of
564 *Dictyostelium.* However, it needs to be ascertained if this particular volatile is ammonia.

565 **Supplementary Results**

566 **Genes involved in autophagy and tipped mound formation do not show altered expression**
567 **in the mutant**

568 Autophagy helps maintain cellular homeostasis by promoting the breakdown of damaged
569 proteins and organelles (Mizushima et al., 2008), and ammonia is recognised to be a diffusible
570 regulator of autophagy in human cells (Eng et al., 2010). To investigate if autophagy is impaired
571 in the mutant, the expression of autophagy markers *atg8* and *atg18* were examined and there was
572 no discernible change in the expression levels when compared to WT (Figure S9A). The tipless
573 to tipped mound transition as well as late developmental gene expression is regulated by *gbf*A, a
574 G-box binding factor (GBF). However, in the *adgf* mutant the *gbf*A expression levels were
575 comparable with no significant difference between the WT at 16 h (Figure S9B). Without the
576 assay for autophagy as well as assay for GBF activity, these expression studies alone are not
577 conclusive to rule out the role of these factors in tip formation.

578 **ADA does not deaminate cytokinin:** ADA is known to interact with 5'AMP (Hanif et al., 2022)
579 and in *Dictyostelium*, 5′-AMP serves as a direct precursor of cytokinin, playing a significant role
580 in cellular signaling and development (Taya et al., 1978). Although docking studies suggest that
581 binding of ADGF with cytokinins (zeatin, dihydrozeatin, isopentenyl adenine) is moderate, (data
582 not shown), we carried a functional assay by mixing cytokinin and ADA with KK2 buffer in one
583 side of the Petridish and found no rescue of the mutant (Figure S10) in such conditions
584 suggesting no functional activity between ADA and cytokinin.

585

586

587 **Supplementary discussion**

588 **Plausible routes of caffeine action rescuing the mound arrest phenotype**

589 The *adgf* mound arrest could be rescued by the addition of the adenosine antagonist, caffeine but
590 treatment with the *pde4* inhibitor, IBMX failed to rescue the mound arrest. Caffeine is known to
591 reduce adenosine levels in blood plasma (Conlay et al., 1988) and also increase ammonium
592 levels in urine samples of rabbits (Bernheim and Bernheim, 1945). Thus, the mound rescue upon
593 caffeine treatment may be a result of reduced adenosine and increased ammonia levels. With
594 respect to caffeine action on cAMP levels, the reports are contradictory. Caffeine has been
595 reported to increase adenylate cyclase expression thereby increasing cAMP levels (Hagmann,
596 1986) whereas Alvarez-Curto et al., (2007) found that caffeine reduced intracellular cAMP levels
597 in *Dictyostelium*. Although, caffeine is moderately potent in inhibiting PDE enzyme activity, the
598 *in vivo* concentrations are likely to be low to be associated with effective PDE inhibition (Burg
599 and Werner, 1975; Daly, 1993).

600 **Material and Methods**

601 **Bioinformatic analyses of ADGF**

602 The genomic sequence and the protein sequence of ADGF were obtained either from dictybase
603 (http://dictybase.org) or NCBI database (https://www.ncbi.nlm.nih.gov/). Within the
604 *Dictyostelium* ADGF, the ADA domain was identified by SMART and BLAST
605 (http://smart.embl-heidelberg.de/) (https://blast.ncbi.nlm.nih.gov/Blast.cgi) (Altschul et al., 1990;
606 Letunic and Bork, 2018) analyses. A phylogenetic tree was generated by aligning multiple amino
607 acid sequences of ADGF from several taxa. Neighbour Joining approach and the MUSCLE
608 alignment tool of the MEGAX programme were used for constructing the tree (Saitou and Nei,
609 1987). The tertiary structure of ADGF was obtained using the online programme alphafold

610 (https://alphafold.ebi.ac.uk/) (Jumper et al., 2021), and PyMol was used for viewing the images.
611 The expression profiles of *ada* and *ada2* during mouse and human gastrula development were
612 retrieved from the marionilab.cruk.cam.ac.uk/MouseGastrulation2018/ and human-gastrula.net/
613 databases (Pijuan-Sala et al., 2019; Tyser et al., 2021), respectively. Protein-protein docking was
614 carried out using High Ambiguity Driven Protein-Protein Docking (HADOCK) version 2.4.

615 **Culture and development of *Dictyostelium discoideum***

616 *D. discoideum* (WT-AX4) cells or the mutant *adgf* derived from AX4, (DBS0237637) were
617 cultured in modified maltose-HL5 medium (Formedium, UK) with 100,000 U/L penicillin and
618 0.1 g/L streptomycin. Three independent insertional mutants (GWDI_17_D_7, GWDI_47_C_1,
619 GWDI_132_H_3) in the *adgf* gene (insertion in exon 2 in all three mutants) were obtained from
620 the GWDI bank (https://remi-seq.org), in *Dictyostelium* stock centre, North Western University,
621 USA (Gruenheit et al., 2021). The mound defects were identical in all three and GWDI_47_C_1
622 alone was characterised further. The culture was raised as a monolayer in Petri plates or grown in
623 an Erlenmeyer flask in shaking conditions at 150 rpm and 22 °C, to a cell density of 2-4x10^6
624 cells/ml. The cells were also grown on SM/5 agar plates supplemented with *Klebsiella aerogenes*
625 at 22 °C (2 g/L glucose, 2 g/L protease peptone, 0.4 g/L yeast extract, 1 g/L $MgSO_4.H_2O$, 0.66
626 g/L K_2HPO_4, 2.225 g/L KH_2PO_4, 1% Bactoagar, pH 6.4). For developmental assays, freshly
627 starved cells were washed twice with ice cold KK2 buffer (2.25 g KH_2PO_4 and 0.67 g K_2HPO_4
628 per litre, pH 6.4), and plated on 1% non-nutrient KK2 agar plates at a density of 5x10^5 cells/cm^2
629 (Nassir et al., 2019). Thereafter, the plates were incubated in dark conditions at 22 °C for
630 development.

631

632 ***Dictyostelium* genomic DNA isolation**

633 WT and *adgf* $^{-}$ cells grown axenically were harvested, and the pellet was resuspended in 1 ml of
634 lysis buffer (50 mM Tris-Cl, pH 8; 10 mM EDTA; 0.8% SDS). To this mixture, 200 µl of
635 Nonidet P-40 (NP40), a non-ionic detergent, was added, vortexed and centrifuged at 12,000 g for
636 15 min at room temperature (RT). The resultant pellet was gently vortexed, resuspended in 500
637 µl of lysis solution containing 200 µg/ml Proteinase K, and incubated at 65 °C for 30 min. 300 µl
638 of phenol: chloroform was added to this suspension, centrifuged at 18,000 g for 10 min at RT,
639 and the resultant aqueous phase was extracted carefully. An equal amount of chloroform was
640 added and centrifuged at 18,000 g for 10 min at RT. Following this, 750 µl of pure ethanol was
641 added to the suspension, which was then centrifuged at 12,000 g for 15 min at 4 °C. Genomic
642 DNA was precipitated by adding twice the volume of absolute ethanol and 1/10th the volume of 3
643 M sodium acetate. After a 10 min centrifugation at 15,000 g, the pellet was cleaned using 70%
644 ethanol and stored at 4 °C. Electrophoresis was conducted in TAE buffer at 50 V using a Medox
645 power pack system (India), and the integrity of DNA was confirmed on a 1% agarose gel.

646 **Validation of the *adgf* mutant**

647 To validate the blasticidin (*bs*r) cassette insertion in the adgf mutant, WT and *adgf* $^{-}$ genomic
648 DNA were isolated, and a diagnostic PCR was performed using the gene and *bsr* insert specific
649 primers in accordance with the guidelines provided in the GWDI website. A qRT-PCR was
650 carried out to confirm the absence of *adgf* expression in the mutant cells. The primers used for
651 mutant validation are listed in Supplementary Table S2.

652 **Quantitative real-time PCR (qRT-PCR)**

653 Total RNA was extracted from WT and *adgf* $^{-}$ cells using Trizol reagent (Favorgen, USA) at
654 specified intervals (every four hours from 0 to 24 h). cDNA was synthesized from the total RNA

655 using a PrimeScript 1st Strand cDNA Synthesis Kit (Takara, Japan). Random primers from the
656 manufacturer were used to generate the cDNA from a template of 1 µg total RNA. qRT-PCR
657 was performed using SYBR Green Master Mix (Thermo Scientific, USA) and 1 µl of cDNA.
658 The expression levels of *adgf*, *acaA*, cAMP receptor A (*carA*), phosphodiesterases (*pdsA*, *regA*),
659 5' nucleotidase (*5'nt*), extracellular matrix A (*ecmA*), extracellular matrix B (*ecmB*), prespore A
660 (*pspA*), countin (*ctn*), and small aggregate (*smlA*) were quantified with a QuantStudio Flex 7
661 (Applied Biosystems, USA). The mitochondrial large RNA subunit (*rnlA*) served as an internal
662 control. qRT-PCR data analysis was conducted according to the method described by Schmittgen
663 and Livak (2008). The primer sequences used for qRT-PCR are provided in Supplementary
664 Table S4.

665 **Generation of *adgf* over expression construct**

666 The full-length 1.7 kb *adgf* sequence was PCR-amplified using ExTaq polymerase (Takara,
667 Japan) with WT genomic DNA as the template. The amplified product was then ligated into the
668 pDXA-GFP2 vector at the HindIII and KpnI restriction sites. Both *adgf* $^-$ and WT cells were
669 electroporated with this vector, and G418-resistant clones (10 µg/ml) were isolated for further
670 analysis. The expression of *adgf* was confirmed by semi-quantitative PCR. The corresponding
671 primer sequences are listed in Supplementary Table S3.

672 **Transformation of *Dictyostelium discoideum***

673 WT and *adgf* $^-$ cells grown axenically were harvested, washed twice with ice-cold EP buffer (10
674 mM KH_2PO_4, 10 mM K_2HPO_4, 50 mM sucrose, pH 6.2), and resuspended in 100 µl of EP++
675 solution (10 K_2HPO_4 mM, 10 mM KH_2PO_4, 50 mM sucrose, 1 mM $MgSO_4$, 1 mM $NaHCO_3$, 1
676 mM ATP, 1 µM $CaCl_2$) containing 10 µg of plasmid vector (Nassir et al., 2019) in pre-cooled
677 cuvettes (BioRad, USA). The cells were electroporated using a BTX ECM830 electroporator

678 (Harvard Apparatus, USA) at 300 V with 2 ms pulses and five square wave pulses at 5-second
679 intervals. The cells were then transferred to a Petri dish with 10 ml of HL5 medium and
680 incubated at 22 °C. After 24 hours, G418 (10 µg/ml) was added to the medium, and resistant
681 colonies were selected for further analysis.

682 **Preparation of conditioned media (CM)**

683 WT and *adgf* $^{-}$ cells grown in HL5 medium were collected at the mid-log (ML) phase,
684 resuspended in KK2 buffer at a density of $1x10^7$ cells/ml, and incubated at 22 °C with shaking
685 for 20 hours. The clarified supernatant obtained after centrifugation was used for the experiments.

686 **Assay for ADA activity**

687 The total ADA activity from *Dictyostelium* was determined as per the protocol of the
688 manufacturer (Abcam, USA; Cat No: ab204695). For sample preparation, $5x10^5$ cells/cm^2 were
689 seeded onto KK2 agar plates and at the mound stage, ice cold ADA assay buffer was flooded,
690 then vigorously pipetted to disrupt the mound integrity. The cell homogenate was agitated on a
691 rotary shaker at 4 °C for 15 min and then centrifuged at 12,000 rpm for 10 min in a cold
692 microfuge tube. The supernatant was subjected to the ADA assay. This ADA test detects inosine,
693 generated from adenosine break down through a multi-step reaction. The intermediate formed
694 combines with the probe to produce uric acid, which is quantified at OD 293 nm. BCA
695 (Bicinchonic acid) assay kit (Thermoscientific, USA) was used for determining the protein
696 concentration. One unit of ADA activity is defined as the amount of enzyme that hydrolyses
697 adenosine to yield 1 µmol of inosine per min under the assay conditions.

698

699

700 **Adenosine quantification**

701 Total adenosine levels from *Dictyostelium* mounds were measured according to the protocol
702 using the Adenosine Assay Kit (Abcam, USA; Cat No: ab211094). Cells grown in HL5 were
703 collected, washed and plated on KK2 agar plates. The lysis buffer was added to the plates with
704 mounds and mixed thoroughly. 50 µl of the lysate was mixed with 2 U of ADA and was
705 subjected to incubation for 15 min at RT. Adenosine quantification involves the use of ADA and
706 after a series of enzymatic reactions, an intermediate is formed which reacts with the adenosine
707 probe generating a fluorescent product. Using a spectrofluorometer (Perkin Emer, USA; λEx =
708 544 nm/λEm = 590), the fluorescence intensity can be measured which is proportional to the
709 concentration of adenosine (Perkin Emer, USA; λEx = 544 nm/λEm = 590). The adenosine
710 levels were quantified using the adenosine standard curve.

711 **Quantification of ammonia**

712 Ammonia assay kit (Sigma-Aldrich, USA; Cat No: AA0100) was used for estimating the total
713 ammonia levels. WT and *adgf* $^{-}$ cells developed on KK2 agar plates were sealed with parafilm
714 and incubated at 22 °C. The mounds were collected using lysis solution, and the debris was
715 removed by centrifugation at 10,000 g for 10 min. The supernatant was used for further analysis.
716 For the ammonia assay, 1 ml of assay reagent was mixed thoroughly with either 100 µl of
717 samples or standards, incubated for 5 min at RT, and the absorbance was measured at 340 nm.
718 Then, 10 µl of L-glutamate dehydrogenase (GDH) solution was added to each cuvette, and after
719 a 5-min incubation at 25 °C, the absorbance was measured again at 340 nm using a
720 spectrophotometer (Eppendorf, Germany). In the presence of GDH, ammonia combines with α-
721 ketoglutaric acid and reduced NADPH to produce L-glutamate and oxidised NADP+. The

722 decrease in absorbance at 340 nm is proportional to the ammonia concentration. The ammonia
723 standard curve was used to calculate the ammonia levels.

724 **Volatile ammonia generation**

725 To generate ammonia, 1 ml of 1 N NaOH and 1 ml of NH_4Cl (concentrations used 0.1 mM, 1
726 mM, 10 mM) were mixed thoroughly (Thadani et al., 1977; Feit et al., 1990) and from this mix,
727 2 ml was aliquoted in the upper half of the Petri dish. The other half of the plate with the *adgf*$^-$
728 mounds on KK2 agar were inverted, sealed and incubated at 22 °C. To determine whether WT
729 mounds, physically separated from the mutants could rescue the mound arrest, WT ($1x10^6$
730 cells/cm^2) and *adgf*$^-$ ($5x10^5$ cells/cm^2) cells were developed on KK2 agar plates on either side of
731 compartmentalised and sealed Petri plates. *adgf*$^-$ cells developed on either side of the dish
732 served as controls.

733 **Quantification of cAMP**

734 Using the cAMP-XP test kit and following the manufacturer's instructions, total cAMP levels
735 were determined from both the WT and the mutant (Cell signaling, USA). WT and *adgf*$^-$
736 mounds were disrupted and collected in 1 ml ice cold KK2 buffer. After centrifuging the pellet,
737 100 µl of 1X lysis solution was added, and the mixture was allowed to rest on ice for 10 min.
738 Following that, 50 µl of lysate and 50 µl of HRP-conjugated cAMP solution were added to the
739 test plates, which were then shaken horizontally at RT. After a 3-hour incubation, the wells were
740 emptied and washed three times with 200 µl of 1X wash buffer. 100 µl of stop solution was
741 added to halt the reaction, and the absorbance was measured at 450 nm using a
742 spectrophotometer (Biorad, USA). The cAMP standard curve was used to determine the cAMP
743 levels.

744 **Visualisation of cAMP waves using dark field optics**

745 $5x10^5$ cells/cm^2 were developed on KK2 agar plates under moist, dark conditions to monitor the
746 propagation of the cAMP wave. Using a Nikon DS-5MC camera mounted on a Nikon SMZ-
747 1000 stereo zoom microscope, a time-lapse video of the aggregation was captured in real-time
748 (Nikon, Japan). cAMP optical density waves were displayed by subtracting the image pairs
749 (Siegert and Weijer, 1995) after processing the images with the NIS-Elements D program or
750 ImageJ (NIH, USA).

751 **Under agarose cAMP chemotaxis assay**

752 The under-agarose cAMP chemotaxis assay (Woznica and Knecht, 2006; Singh and Insall, 2022)
753 was carried out with cells obtained from WT and *adgf*$^-$ mounds. Briefly, the cells were starved
754 in KK2 buffer at $1x10^7$ cells/ml density. Three parallel troughs, each measuring 2 mm in width,
755 were set up on a Petri dish containing 1% agarose. In the outer two troughs, 100 µl of WT and
756 *adgf*$^-$ cell suspension was aliquoted respectively and 10 µM cAMP was added to the central
757 trough. Cell migration toward cAMP was recorded every 30 s over a total duration of 20 min
758 using the NIS-Elements D software and an inverted Nikon Eclipse TE2000 microscope (Nikon,
759 Japan). 35 cells were tracked each time and subsequently analysed using ImageJ (NIH, USA).

760 **Reconstitution of WT with mutant cells**

761 WT and *adgf*$^-$ cells cultured in HL5 medium, were harvested at the ML phase by centrifugation,
762 rinsed twice with ice-cold KK2 buffer. The cells mixed in different ratios (1:9, 2:8 and 1:1) were
763 adjusted to a final density of $5x10^5$ cells/cm^2, plated on 1% KK2 agar plates, and incubated at
764 22 °C for development.

765

766 **Tracking cell fate after reconstitution**

767 *Dictyostelium* cells harvested from fresh HL5 media were resuspended at a density of $1x10^6$
768 cells/ml in KK2 buffer, followed by incubation at 22°C for 1.5 h in shaking conditions with 0.2
769 µM DIL, (1,1'-Dioctadecyl-3,3,3',3'-Tetramethylindocarbocyanine Perchlorate, Invitrogen, USA)
770 a cell tracker dye. DIL has been used extensively as a cell tracker in *C. elegans*, *Xenopus and*
771 mice (Schultz and Gumienny, 2012; Xu et al., 2020; Erdogan et al., 2016). WT or *adgf*$^-$ cells
772 labelled with DIL were reconstituted with the unlabelled cells in a ratio of 1:9, 2:8 and 1:1 and
773 plated for development. In the ratios mentioned, the smaller fraction represents the stained cells.
774 DIL is a lipophilic dye that selectively stains the plasma membranes of living cells, allowing
775 visualization and analysis of cell morphology.

776 **Neutral red staining of mounds and slugs**

777 WT and *adgf*$^-$ cells harvested from HL5 cultures were resuspended at a density of $1x10^7$ cells
778 per ml in KK2 buffer and treated with 0.005% neutral red (NR) solution for 15 min at RT in
779 shaking conditions (Bonner, 1952). The stained cells were washed twice with KK2 buffer, plated
780 in buffered agar plates and thereafter, NR stained slugs were observed using an upright
781 microscope.

782 **Cell-cell adhesion assay**

783 After 14 h of development on phosphate buffered agar plates, WT and *adgf*$^-$ mounds were
784 disaggregated by repeated pipetting and vortexing using ice-cold KK2 buffer. Dissociated cells
785 were resuspended in KK2 buffer and incubated at 150 rpm for 45 min. Single and non-adherent
786 cells were counted using a Neubauer chamber (Lam et al., 1981).

787

788 **Treatment of *Dictyostelium* cells with different compounds**

789 A highly specific ADA inhibitor, DCF that inhibits both extra and intra-cellular ADAs (Cha et
790 al., 1975) was mixed with the WT cell suspension and plated on 1% non- nutrient KK2 agar
791 plates at a density of $5x10^5$ cells/cm^2. Of the different DCF concentrations tested (10 nM, 50 nM,
792 100 nM and 1 μM), 100 nM showed complete tip inhibition.

793 For the enzymatic rescue assay, 10 U of bovine ADA dissolved in KK2 buffer (Sigma-Aldrich,
794 USA) was added onto mutant mounds. The concentrations of 8-Br-cAMP (2 mM), cAMP (0.1
795 mM, 0.5 mM), c-di-GMP (0.1 mM, 0.5 mM), adenosine (1 μM, 10 μM, 100 μM, 1 mM),
796 caffeine (10 nM, 100 nM, 1 μM) and IBMX (3-isobutyl-1-methylxanthine 0.5 mM) were based
797 on previous publications (Chen et al., 2017; Chen and Schaap, 2012; Nassir et al., 2019; Siegert
798 and Weijer, 1989) and these compounds were added independently either on top of the mounds
799 or supplemented while plating. All the fine chemicals were from Sigma-Aldrich, USA except
800 when mentioned.

801 **Microscopy**

802 Microscopy was performed using a Nikon SMZ-1000 stereo zoom microscope with
803 epifluorescence optics, Nikon 80i Eclipse upright microscope, or a Nikon Eclipse TE2000
804 inverted microscope, connected with a digital sight DS-5MC camera (Nikon). Image processing
805 was carried out using NIS-Elements D (Nikon) or Image J.

806 **Statistical tools**

807 Data analyses were carried out using Microsoft Excel (2016). Statistical significance was
808 determined by paired or unpaired, one-tailed Student's t-test (GraphPad Prism, version 6).

809

810 **Acknowledgements**

811 We gratefully acknowledge the help of NBRP Nenkin, Japan and *Dictyostelium* Stock Center
812 (DSC), Northwestern University, USA for providing various strains and plasmids used in this
813 study. We thank Prof. Richard Gomer, Texas A&M, USA for providing *aprA* mutant strain. We
814 thank Prof. Kei Inouye, Kyoto University, Japan and Prof. Kees Weijer, University of Dundee,
815 UK for their comments on an earlier version of the manuscript.

816 **Author contributions**

817 P.H. and R.B. conceptualized the work. P.H. performed all experiments. P.H. and R.B. analysed
818 the data and wrote the manuscript.

819 **Competing interests**

820 The authors declare no competing interests.

821 **References**

822 Aoki, M. M., Emery, R. J., Anjard, C., Brunetti, C. R., and Huber, R. J. (2020). Cytokinins in
823 *Dictyostelia*–A unique model for studying the functions of signaling agents from species to
824 kingdoms. *Frontiers in Cell and Developmental Biology*, 511.

825 Altschul, S. F., Gish, W., Miller, W., Myers, E. W. and Lipman, D. J. (1990). Basic local
826 alignment search tool. *J. Mol. Biol.* 215, 403–410.

827 Alvarez-Curto, E., Weening, K. E., and Schaap, P. (2007). Pharmacological profiling of the
828 *Dictyostelium* adenylate cyclases ACA, ACB and ACG. *Biochemical Journal*, 401(1), 309-316.

829 Anjard, C., and Loomis, W. F. (2003). Histidine kinases of *Dictyostelium*. In *Histidine Kinases*
830 *in Signal Transduction* (pp. 421-438). Academic Press.

831 Annesley, S. J., and Fisher, P. R. (2009). *Dictyostelium discoideum*—a model for many
832 reasons. *Molecular and Cellular Biochemistry*, 329, 73-91.

833 Bader, S., Kortholt, A., and Van Haastert, P. J. (2007). Seven *Dictyostelium discoideum*
834 phosphodiesterases degrade three pools of cAMP and cGMP. *Biochemical Journal*, 402(1), 153-
835 161.

836 Bagorda, A., Das, S., Rericha, E. C., Chen, D., Davidson, J., and Parent, C. A. (2009). Real-time
837 measurements of cAMP production in live *Dictyostelium* cells. *Journal of Cell Science*, 122(21),
838 3907-3914.

839 Bernheim, F., and Bernheim, M. L. (1945). Note on the effect of caffeine on ammonia and urea
840 excretion in rabbits. *American Journal of Physiology-Legacy Content*, 145(1), 115-117.

841 Bloom, L., and Kay, R. R. (1988). The search for morphogenes in *Dictyostelium*. *Bioessays*, 9(6),
842 187-191.

843 Bonner, J. T. (2008). *The social amoebae: the biology of cellular slime molds*. Princeton
844 University Press. USA.

845 Bonner, J. T., Suthers, H. B., and Odell, G. M. (1986). Ammonia orients cell masses and speeds
846 up aggregating cells of slime moulds. *Nature*, 323(6089), 630-632.

847 Bonner, J. T., and Hoffman, M. E. (1963). Evidence for a substance responsible for the spacing
848 pattern of aggregation and fruiting in the cellular slime molds. *Development*, 11(3), 571-589.

849 Bose, S. et al., (2020). tRNA adenosine deaminase 3 is required for telomere maintenance in
850 *Arabidopsis thaliana*. *Plant Cell Reports*, 39, 1669-1685.

851 Bradbury, J. M., and Gross, J. D. (1989). The effect of ammonia on cell-type-specific enzyme
852 accumulation in *Dictyostelium discoideum*. *Cell Differentiation and Development*, 27(2), 121-
853 128.

854 Brady, T. G., and Hegarty, V. J. (1966). An investigation of plant seeds for adenosine
855 deaminase. *Nature*, 209(5027), 1027-1028.

856 Brock, D. A., and Gomer, R. H. (1999). A cell-counting factor regulating structure size in
857 *Dictyostelium*. *Genes and Development*, 13(15), 1960-1969.

858 Brock, D. A., Ehrenman, K., Ammann, R., Tang, Y., and Gomer, R. H. (2003). Two components
859 of a secreted cell number-counting factor bind to cells and have opposing effects on cAMP
860 signal transduction in *Dictyostelium*. *Journal of Biological Chemistry*, 278(52), 52262-52272.

861 Burg, A. W., and Werner, E. (1975). Effect of orally-administered caffeine and theophylline on
862 tissue concentrations of 3', 5'cyclic-amp and phospho-diesterase. *Federation Proceedings,* 34(3),
863 332-332.

864 Carpousis, A. J., Vanzo, N. F., and Raynal, L. C. (1999). mRNA degradation: a tale of poly (A)
865 and multiprotein machines. *Trends in Genetics*, 15(1), 24-28.

866 Carrin, I., Murgia, I., McLachlan, A., and Kay, R. R. (1996). A mutational analysis of
867 *Dictyostelium discoideum* multicellular development. *Microbiology*, 142(4), 993-1003.

868 Cha, S., Agarwal, R. P., and Parks Jr, R. E. (1975). Tight-binding inhibitors—II: Non-steady
869 state nature of inhibition of milk xanthine oxidase by allopurinol and alloxanthine and of human

870 erythrocytic adenosine deaminase by coformycin. *Biochemical Pharmacology*, 24(23), 2187-
871 2197.

872 Chen, Z. H., and Schaap, P. (2012). The prokaryote messenger c-di-GMP triggers stalk cell
873 differentiation in *Dictyostelium*. *Nature*, 488(7413), 680-683.

874 Chen, Z. H., and Schaap, P. (2016). Secreted cyclic di-GMP induces stalk cell differentiation in
875 the eukaryote *Dictyostelium discoideum*. *Journal of Bacteriology*, 198(1), 27-31.

876 Chen, Z. H., Singh, R., Cole, C., Lawal, H. M., Schilde, C., Febrer, M., Barton, G. J. and Schaap,
877 P. (2017). Adenylate cyclase A acting on PKA mediates induction of stalk formation by cyclic
878 diguanylate at the *Dictyostelium* organizer. *Proceedings of the National Academy of Sciences*
879 *(USA)*, 114(3), 516-521.

880 Chien, S., Chung, C. Y., Sukumaran, S., Osborne, N., Lee, S., Ellsworth, C., Mc Nally, G. Y.,
881 and Firtel, R. A. (2000). The *Dictyostelium* LIM domain-containing protein LIM2 is essential for
882 proper chemotaxis and morphogenesis. *Molecular Biology of the Cell*, *11*(4), 1275-1291.

883 Cristalli, G., Costanzi, S., Lambertucci, C., Lupidi, G., Vittori, S., Volpini, R., and Camaioni, E.
884 (2001). Adenosine deaminase: functional implications and different classes of
885 inhibitors. *Medicinal Research Reviews*, 21(2), 105-128.

886 Coates, J. C., and Harwood, A. J. (2001). Cell-cell adhesion and signal transduction during
887 *Dictyostelium* development. *Journal of Cell Science*, 114(24), 4349-4358.

888 Conlay, L. A., Evoniuk, G., and Wurtman, R. J. (1988). Endogenous adenosine and hemorrhagic
889 shock: effects of caffeine administration or caffeine withdrawal. *Proceedings of the National*
890 *Academy of Sciences (USA)*, 85(12), 4483-4485.

891 Cotter, D. A., Dunbar, A. J., Buconjic, S. D., and Wheldrake, J. F. (1999). Ammonium
892 phosphate in sori of *Dictyostelium discoideum* promotes spore dormancy through stimulation of
893 the osmosensor ACG. *Microbiology*, 145(8), 1891-1901.

894 Daly, J. W. (1993). Mechanism of action of caffeine. *Caffeine, coffee, and health*, 97-150. Raven
895 press.

896 Davies, L., Satre, M., Martin, J. B., and Gross, J. D. (1993). The target of ammonia action in
897 *Dictyostelium*. *Cell*, 75(2), 321-327.

898 Dolezal, T., Dolezelova, E., Zurovec, M., and Bryant, P. J. (2005). A role for adenosine
899 deaminase in *Drosophil*a larval development. *PLoS Biology*, 3(7), e201.

900 Dunn, J. D., Bosmani, C., Barisch, C., Raykov, L., Lefrancois, L. H., Cardenal-Munoz, E., et al.
901 (2018). Eat prey, live: *Dictyostelium discoideum* as a model for cell-autonomous
902 defenses. *Frontiers in Immunology*, 8, 1906.

903 Eichinger L et al., (2005). The genome of the social amoeba *Dictyostelium discoideum*. *Nature*.
904 435(7038):43-57.

905 Eidhammer, I., Jonassen, I., and Taylor, W. R. (2000). Structure comparison and structure
906 patterns. *Journal of Computational Biology*, *7*(5), 685-716.

907 Eng, C. H., Yu, K., Lucas, J., White, E., and Abraham, R. T. (2010). Ammonia derived from
908 glutaminolysis is a diffusible regulator of autophagy. *Science signaling*, 3(119).

909 Erdogan, B., Ebbert, P. T., and Lowery, L. A. (2016). Using *Xenopus laevis* retinal and spinal
910 neurons to study mechanisms of axon guidance in vivo and in vitro. *Seminars in Cell and*
911 *Developmental Biology,* 51, 64-72. Academic Press. USA.

912 Farnsworth, P. (1973). Morphogenesis in the cellular slime mould *Dictyostelium discoideum*; the
913 formation and regulation of aggregate tips and the specification of developmental axes.
914 *Development,* 29(2), 253-266.

915 Feit, I. N. (1988). Ammonia can stimulate or inhibit aggregate density in *Dictyostelium*
916 *mucoroides*: A quantitative test of the hypothesis that ammonia is the aggregation-suppressing
917 gas. *Developmental Genetics*, 9(4-5), 639-652.

918 Feit, I. N., Medynski, E. J., and Rothrock, M. J. (2001). Ammonia differentially suppresses the
919 cAMP chemotaxis of anterior-like cells and prestalk cells in *Dictyostelium discoideum*. *Journal*
920 *of Biosciences*, 26, 157-166.

921 Felsenstein, J. (1985). Confidence limits on phylogenies: an approach using the
922 bootstrap. *Evolution*, 39(4), 783-791.

923 Firtel, R. A. (1996). Interacting signaling pathways controlling multicellular development in
924 *Dictyostelium*. *Current Opinion in Genetics and Development*, 6(5), 545-554.

925 Follstaedt, S. C., Kirsten, J. H., and Singleton, C. K. (2003). Temporal and spatial expression of
926 ammonium transporter genes during growth and development of *Dictyostelium*
927 *discoideum. Differentiation*, 71(9-10), 557-566.

928 Gaspar, H. B. (2010). Bone marrow transplantation and alternatives for adenosine deaminase
929 deficiency. *Immunology and Allergy Clinics*, 30(2), 221-236.

930 Gee, K., Russell, F., and Gross, J. D. (1994). Ammonia hypersensitivity of slugger mutants of D.
931 discoideum. *Journal of Cell Science*, 107(2), 701-708.

932 Gruenheit, N. et al., (2021). Mutant resources for functional genomics in *Dictyostelium*
933 *discoideum* using REMI-seq technology. *BMC Biology*, 19(1), 172.

934 Hagmann, J. (1986). Caffeine and heat shock induce adenylate cyclase in *Dictyostelium*
935 *discoideum*. *The EMBO Journal*, 5(13), 3437-3440.

936 Hames, B. D., and Ashworth, J. M. (1974). The metabolism of macromolecules during the
937 differentiation of myxamoebae of the cellular slime mould *Dictyostelium discoideum* containing
938 different amounts of glycogen. *Biochemical Journal*, 142(2), 301-315.

939 Hanif, M. A., Hossen, S., Cho, Y., Sukhan, Z. P., Choi, C. Y., and Kho, K. H. (2022).
940 Characterization and expression analysis of mollusk-like growth factor: A secreted protein
941 involved in Pacific abalone embryonic and larval development. *Biology*, 11(10), 1445.

942 Harrison, M. J. (2005). signaling in the arbuscular mycorrhizal symbiosis. *Annu. Rev. Microbiol*.,
943 59, 19-42.

944 Helgason, T., Daniell, T. J., Husband, R., Fitter, A. H., and Young, J. P. W. (1998). Ploughing up
945 the wood-wide web. *Nature*, 394(6692), 431-431.

946 Hiraoka, H., Wang, J., Nakano, T., Hirano, Y., Yamazaki, S., Hiraoka, Y., and Haraguchi, T.
947 (2022). ATP levels influence cell movement during the mound phase in *Dictyostelium*
948 *discoideum* as revealed by ATP visualization and simulation. *FEBS Open bio*, 12(11), 2042-2056.

949 Honorato, R. V., Koukos, P. I., Jiménez-García, B., Tsaregorodtsev, A., Verlato, M., Giachetti,
950 A., Rosato, A., and Bonvin, A. M. (2021). Structural biology in the clouds: the WeNMR-EOSC
951 ecosystem. *Frontiers in Molecular Biosciences*, 8, 729513.

952 Honorato, R. V., Trellet, M. E., Jiménez-García, B., Schaarschmidt, J. J., Giulini, M., Reys, V.,
953 Koukos, P. I., Rodrigues, J. P. G. L. M., Karaca, E., van Zundert, G. C. P., Roel-Touris, J., van
954 Noort, C. W., Jandova, Z., Melquiond, A. S. J., and Bonvin, A. M. (2024). The HADDOCK2. 4
955 web server for integrative modeling of biomolecular complexes. *Nature Protocols*, 1-23.

956 Huber, R. J., Williams, R. S., and Müller-Taubenberger, A. (2022). *Dictyostelium*: A Tractable
957 Cell and Developmental Model in Biomedical Research. *Frontiers in Cell and Developmental*
958 *Biology*, 10, 909619.

959 Iijima, R., Kunieda, T., Yamaguchi, S., Kamigaki, H., Fujii-Taira, I., Sekimizu, K., Kubo, T.,
960 Natori, S., Homma, K. J. (2008). The extracellular adenosine deaminase growth factor,
961 ADGF/CECR1, plays a role in *Xenopus* embryogenesis via the adenosine/P1 receptor. *J Biol*
962 *Chem*. 283(4):2255–2264.

963 Inouye, K. (1989). Control of cell type proportions by a secreted factor in *Dictyostelium*
964 *discoideum*. *Development*, 107(3), 605-609.

965 Jumper, J et. al., (2021). Highly accurate protein structure prediction with
966 alphafold. *Nature*, 596(7873), 583-589.

967 Kay, R. R., Tilly, R., and Garrod, D. (1978). Requirement for cell differentiation in
968 *Dictyostelium discoideum*. *Nature*, 271(5640), 58-60.

969 Kellerman, K. A., and McNally, J. G. (1999). Mound-Cell Movement and Morphogenesis in
970 *Dictyostelium*. *Developmental Biology*, *208*(2), 416-429.

971 Kessin, R. H. (2001). *Dictyostelium*: evolution, cell biology, and the development of
972 multicellularity (Vol. 38). Cambridge University Press.

973 Khachatrian, L., Klein, C., and Howlett, A. (1987). Regulation of *Dictyostelium discoideum*
974 adenylate cyclase by manganese and adenosine analogs. *Biochimica et Biophysica Acta (BBA)-*
975 *Molecular Cell Research*, 927(2), 235-246.

976 Kirsten, J. H., Xiong, Y., Dunbar, A. J., Rai, M., and Singleton, C. K. (2005). Ammonium
977 transporter C of *Dictyostelium discoideum* is required for correct prestalk gene expression and
978 for regulating the choice between slug migration and culmination. *Developmental*
979 *Biology*, 287(1), 146-156.

980 Koehl, P. (2001). Protein structure similarities. *Current Opinion in Structural Biology*, 11(3),
981 348-353.

982 Konijn, T. M., Van De Meene, J. G., Bonner, J. T., and Barkley, D. S. (1967). The acrasin
983 activity of adenosine-3', 5'-cyclic phosphate. *Proceedings of the National Academy of Sciences*
984 *(USA)*, 58(3), 1152-1154.

985 Kosugi, T., and Inouye, K. (1989). Negative chemotaxis to ammonia and other weak bases by
986 migrating slugs of the cellular slime moulds. *Microbiology*, 135(6), 1589-1598.

987 Kumar, S., Stecher, G., Li, M., Knyaz, C., and Tamura, K. (2018). MEGA X: molecular
988 evolutionary genetics analysis across computing platforms. *Molecular Biology and*
989 *Evolution*, 35(6), 1547.

990 Lam, T., Pickering, G., Geltosky, J., and Siu, C. H. (1981). Differential cell cohesiveness
991 expressed by prespore and prestalk cells of *Dictyostelium discoideum*. *Differentiation*, *20*(1-3),
992 22-28.

993 Lane, M., and Gardner, D. K. (2003). Ammonium induces aberrant blastocyst differentiation,
994 metabolism, pH regulation, gene expression and subsequently alters fetal development in the
995 mouse. *Biology of Reproduction*, 69(4), 1109-1117.

996 Letunic, I., and Bork, P. (2018). 20 years of the SMART protein domain annotation
997 resource. *Nucleic Acids Research*, 46(D1), D493-D496.

998 Lipkowski, J., and Galus, Z. (1973). Electrode kinetics in mixed solvents Investigations of the
999 kinetics and equilibrium properties of manganese (II)—ammonia complexes in water and mixed
1000 solvents of n-propanol, isopropanol, t-butanol and water. *Journal of Electroanalytical Chemistry*
1001 *and Interfacial Electrochemistry*, 48(3), 337-352.

1002 Liu, Y., Zhang, X., Wang, W., Liu, T., Ren, J., Chen, S., Lu, T., Yuan, X., Mo, F., Yang, J, Wei,
1003 Y., and Wei, X. (2022). Ammonia promotes the proliferation of bone marrow-derived
1004 mesenchymal stem cells by regulating the Akt/mTOR/S6k pathway. *Bone Research*, 10(1), 57.

1005 Lonski, J. (1976). The effect of ammonia on fruiting body size and microcyst formation in the
1006 cellular slime molds. *Developmental Biology*, 51(1), 158-165.

1007 Loomis, W. F., Klein, C., and Bracket, P. (1979). The effect of divalent cations on aggregation of
1008 *Dictyostelium discoideum*. *Differentiation*, 12(1-3), 83-89.

1009 Lu, J., Li, Y., Zhang, C., Yang, X., and Qiang, J. W. (2020). Interaction of manganese and
1010 ammonia in the brain of hepatic encephalopathy rats. *Hepatitis Monthly*, 20(8).

1011 Mahadeo, D. C., and Parent, C. A. (2006). Signal relay during the life cycle of
1012 *Dictyostelium*. *Current topics in Developmental Biology*, *73*, 115-140.

1013 Maier, S. A., Galellis, J. R., and McDermid, H. E. (2005). Phylogenetic analysis reveals a novel
1014 protein family closely related to adenosine deaminase. *Journal of Molecular Evolution*, 61, 776-
1015 794.

1016 Mann, S. K., and Firtel, R. A. (1993). cAMP-dependent protein kinase differentially regulates
1017 prestalk and prespore differentiation during *Dictyostelium* development. *Development*, *119*(1),
1018 135-146.

1019 Marone, G., Plaut, M., and Lichtenstein, L. M. (1980). The role of adenosine in the control of
1020 immune function. *Ricerca in clinica e in laboratorio*., 10(2), 303-312.

1021 Martín-González, J., Montero-Bullón, J. F., and Lacal, J. (2021). *Dictyostelium discoideum* as a
1022 non-mammalian biomedical model. *Microbial Biotechnology*, 14(1), 111-125.

1023 Mizushima, N., Levine, B., Cuervo, A. M., and Klionsky, D. J. (2008). Autophagy fights disease
1024 through cellular self-digestion. *Nature*, 451(7182), 1069-1075.

1025 Moreno, E., Canet, J., Gracia, E., Lluís, C., Mallol, J., Canela, E. I., Cortés. A. and Casadó, V.
1026 (2018). Molecular Evidence of Adenosine Deaminase Linking Adenosine A2A Receptor and
1027 CD26 Proteins. *Frontiers in Pharmacology*, 9, 106.

1028 Müller-Taubenberger, A., Kortholt, A., and Eichinger, L. (2013). Simple system–substantial
1029 share: the use of *Dictyostelium* in cell biology and molecular medicine. *European Journal of Cell*
1030 *Biology*, 92(2), 45-53.

1031 Nassir, N., Hyde, G. J., and Baskar, R. (2019). A telomerase with novel non-canonical roles:
1032 TERT controls cellular aggregation and tissue size in *Dictyostelium*. *PLoS Genetics*, *15*(6),
1033 e1008188.

1034 Nathan Feit, I., Bonner, J. T., and Suthers, H. B. (1990). Regulation of the anterior-like cell state
1035 by ammonia in *Dictyostelium discoideum*. *Developmental Genetics*, 11(5-6), 442-446.

1036 Neave, N., Sobolewski, A., and Weeks, G. (1983). The effect of ammonia on stalk cell formation
1037 in submerged monolayers of *Dictyostelium discoideum*. *Cell Differentiation*, 13(4), 301-307.

1038 Needham, J. (1926). The energy-sources in ontogenesis: III. The ammonia content of the
1039 developing avian egg and the theory of recapitulation. *Journal of Experimental Biology*, 4(2),
1040 145-154.

1041 Newell, P. C., Telser, A., and Sussman, M. (1969). Alternative developmental pathways
1042 determined by environmental conditions in the cellular slime mold *Dictyostelium*
1043 *discoideum*. *Journal of Bacteriology*, 100(2), 763-768.

1044 Newell, P. C. (1982). Cell surface binding of adenosine to *Dictyostelium* and inhibition of
1045 pulsatile signaling. *FEMS Microbiology Letters*, 13(4), 417-421.

1046 Notarangelo, L. D. (2016). T cell immunodeficiencies. *Paediatric Allergy, E-Book: Principles*
1047 *and Practice*, 80-89.

1048 Otto, G. P., Wu, M. Y., Kazgan, N., Anderson, O. R., and Kessin, R. H. (2003). Macroautophagy
1049 is required for multicellular development of the social amoeba *Dictyostelium discoideum*.
1050 *Journal of Biological Chemistry*, 278(20), 17636-17645.

1051 Otto, G. P., Wu, M. Y., Clarke, M., Lu, H., Anderson, O. R., Hilbi, H., Shuman, H, A and Kessin,
1052 R. H. (2004). Macroautophagy is dispensable for intracellular replication of *Legionella*
1053 *pneumophila* in *Dictyostelium discoideum*. *Molecular Microbiology*, *51*(1), 63-72.

1054 Palsson, E., and Cox, E. C. (1996). Origin and evolution of circular waves and spirals in
1055 *Dictyostelium discoideum* territories. *Proceedings of the National Academy of Sciences (USA)*,
1056 93(3), 1151-1155.

1057 Pijuan-Sala, B., Griffiths, J. A., Guibentif, C., Hiscock, T. W., Jawaid, W., Calero-Nieto, F. J.,
1058 Mulas, C., Ibarra-Soria, X., Tyser, R. C. V, Ho, D. L. L., Reik, W., Srinivas, S., Simons, D. B.,
1059 Nichols, J., Marioni, J.C., and Göttgens, B. (2019). A single-cell molecular map of mouse
1060 gastrulation and early organogenesis. *Nature*, 566(7745), 490-495.

1061 Raper, K. B. (1940). Pseudoplasmodium formation and organization in *Dictyostelium*
1062 discoideum. *Journal of the Elisha Mitchell Scientific Society*, 56(2), 241-282.

1063 Riazi, A. M., Arsdell, G. V., and Buchwald, M. (2005). Transgenic expression of CECR1
1064 adenosine deaminase in mice results in abnormal development of heart and kidney. *Transgenic*
1065 *Research*, 14, 333-336.

1066 Riley, B. B., and Barclay, S. L. (1990). Ammonia promotes accumulation of intracellular cAMP
1067 in differentiating amoebae of *Dictyostelium discoideum*. *Development*, 109(3), 715-722.

1068 Rivera-Mancía, S., Ríos, C., and Montes, S. (2012). Manganese and ammonia interactions in the
1069 brain of cirrhotic rats: effects on brain ammonia metabolism. *Neurochemical Research*, 37,
1070 1074-1084.

1071 Roisin-Bouffay, C., Jang, W., Caprette, D. R., and Gomer, R. H. (2000). A precise group size in
1072 *Dictyostelium* is generated by a cell-counting factor modulating cell–cell adhesion. *Molecular*
1073 *Cell*, 6(4), 953-959.

1074 Rubin, J., and Robertson, A. (1975). The tip of the *Dictyostelium discoideum* pseudoplasmodium
1075 as an organizer. *Development*, 33(1), 227-241.

1076 Saitou, N., and Nei, M. (1987). The neighbor-joining method: a new method for reconstructing
1077 phylogenetic trees. *Molecular Biology and Evolution*, 4(4), 406-425.

1078 Saxe, C. 3., Ginsburg, G. T., Louis, J. M., Johnson, R., Devreotes, P. N., and Kimmel, A. R.
1079 (1993). CAR2, a prestalk cAMP receptor required for normal tip formation and late development
1080 of *Dictyostelium discoideum*. *Genes and Development*, 7(2), 262-272.

1081 Schaap, P., Brandt, R., and van Es, S. (1995). Regulation of *Dictyostelium* adenylylcyclases by
1082 morphogen-induced modulation of cytosolic pH or Ca^{2+} levels. *Developmental Biology*, 168(1),
1083 179-188.

1084 Schaap, P., and Wang, M. (1986). Interactions between adenosine and oscillatory cAMP
1085 signaling regulate size and pattern in *Dictyostelium*. *Cell*, 45(1), 137-144.

1086 Schindler, J., and Sussman, M. (1977). Ammonia determines the choice of morphogenetic
1087 pathways in *Dictyostelium discoideum*. *Journal of Molecular Biology*, 116(1), 161-169.

1088 Schindler, J., and Sussman, M. (1979). Inhibition by ammonia of intracellular cAMP
1089 accumulation in *Dictyostelium discoideum*: its significance for the regulation of
1090 morphogenesis. *Developmental Genetics*, 1(1), 13-20.

1091 Schmittgen, T. D., and Livak, K. J. (2008). Analyzing real-time PCR data by the comparative CT
1092 method. *Nature protocols*, 3(6), 1101-1108.

1093 Schulz-Bohm, K., Martín-Sánchez, L., and Garbeva, P. (2017). Microbial volatiles: small
1094 molecules with an important role in intra and inter-kingdom interactions. *Frontiers in*
1095 *Microbiology*, 8, 289291.

1096 Schultz, R. D., and Gumienny, T. L. (2012). Visualization of *Caenorhabditis elegans* cuticular
1097 structures using the lipophilic vital dye DiI. *Journal of Visualized Experiments*, (59), e3362.

1098 Siegert, F., and Weijer, C. (1989). Digital image processing of optical density wave propagation
1099 in *Dictyostelium discoideum* and analysis of the effects of caffeine and ammonia. *Journal of Cell*
1100 *Science*, 93(2), 325-335.

1101 Siegert, F., and Weijer, C. J. (1995). Spiral and concentric waves organize multicellular
1102 *Dictyostelium* mounds. *Current Biology*, 5(8), 937-943.

1103 Singer, G., Araki, T., and Weijer, C. J. (2019). Oscillatory cAMP cell-cell signaling persists
1104 during multicellular *Dictyostelium* development. *Communications Biology*, *2*(1), 139.

1105 Singh, S. P., and Insall, R. H. (2022). Under-Agarose Chemotaxis Chemotaxis and Migration
1106 Assays for *Dictyostelium*. In *Cell Polarity Signaling: Methods and Protocols* (pp. 467-482). New
1107 York, NY: Springer US.

1108 Singleton, C. K., Zinda, M. J., Mykytka, B., and Yang, P. (1998). The histidine kinase dhkC
1109 regulates the choice between migrating slugs and terminal differentiation in *Dictyostelium*
1110 *discoideum*. *Developmental Biology*, 203(2), 345-357.

1111 Singleton, C. K., Kirsten, J. H., and Dinsmore, C. J. (2006). Function of ammonium transporter
1112 A in the initiation of culmination of development in *Dictyostelium discoideum*. *Eukaryotic*
1113 *Cell*, 5(7), 991-996.

1114 Singleton, C. K., and Xiong, Y. (2013). Loss of the histidine kinase DhkD results in mobile
1115 mounds during development of *Dictyostelium discoideum*. *Plos One*, 8(9), e75618.

1116 Siu, C. H., Lam, T. Y., and Choi, A. H. (1985). Inhibition of cell-cell binding at the aggregation
1117 stage of *Dictyostelium discoideum* development by monoclonal antibodies directed against an
1118 80,000-dalton surface glycoprotein. *Journal of Biological Chemistry*, 260(29), 16030-16036.

1119 Steer, M. L. (1975). Adenyl cyclase. *Annals of Surgery*, 182(5), 603.

1120 Stege, J. T., Laub, M. T., and Loomis, W. F. (1999). Tip genes act in parallel pathways of early
1121 *Dictyostelium* development. *Developmental Genetics*, 25(1), 64-77.

1122 Stein, L. Y., Campbell, M. A., and Klotz, M. G. (2013). Energy-mediated vs. ammonium-
1123 regulated gene expression in the obligate ammonia-oxidizing bacterium, *Nitrosococcus oceani*.
1124 *Frontiers in Microbiology*, 4, 277.

1125 Sternfeld, J., and David, C. N. (1982). Fate and regulation of anterior-like cells in *Dictyostelium*
1126 slugs. *Developmental Biology*, 93(1), 111-118.

1127 Storey, C. L., Williams, R. S. B., Fisher, P. R., and Annesley, S. J. (2022). *Dictyostelium*
1128 *discoideum*: A model system for neurological disorders. *Cells*, 11(3), 463.

1129 Tanaka, T., Kameoka, J., Yaron, A., Schlossman, S. F., and Morimoto, C. (1993). The
1130 costimulatory activity of the CD26 antigen requires dipeptidyl peptidase IV enzymatic activity.
1131 *Proceedings of the National Academy of Sciences (USA)*, 90(10), 4586-4590.

1132 Taya, Y., Tanaka, Y., and Nishimura, S. (1978). 5′-AMP is a direct precursor of cytokinin in
1133 *Dictyostelium discoideum*. *Nature*, 271(5645), 545-547.

1134 Thadani, V., Pan, P., and Bonner, J. T. (1977). Complementary effects of ammonia and cAMP
1135 on aggregation territory size in the cellular slime mold *Dictyostelium mucoroides*. *Experimental*
1136 *Cell Research*, 108(1), 75-78.

1137 Theibert, A., and Devreotes, P. N. (1984). Adenosine and its derivatives inhibit the cAMP
1138 signaling response in *Dictyostelium discoideum*. *Developmental Biology*, 106(1), 166-173.

1139 Thomason, P., Traynor, D., and Kay, R. (1999). Taking the plunge: terminal differentiation in
1140 *Dictyostelium*. *Trends in Genetics*, 15(1), 15-19.

1141 Thompson, C. R., and Kay, R. R. (2000). The role of DIF-1 signaling in *Dictyostelium*
1142 *development*. *Molecular Cell*, 6(6), 1509-1514.

1143 Traynor, D., Kessin, R. H., and Williams, J. G. (1992). Chemotactic sorting to cAMP in the
1144 multicellular stages of *Dictyostelium* development. *Proceedings of the National Academy of*
1145 *Sciences (USA)*, 89(17), 8303-8307.

1146 Tung, S. M., Ünal, C., Ley, A., Peña, C., Tunggal, B., Noegel, A. A., Krut, O., Steinert, M., and
1147 Eichinger, L. (2010). Loss of *Dictyostelium* ATG9 results in a pleiotropic phenotype affecting
1148 growth, development, phagocytosis and clearance and replication of *Legionella pneumophila*.
1149 *Cellular Microbiology*, 12(6), 765-780.

1150 Tyser, R. C., Mahammadov, E., Nakanoh, S., Vallier, L., Scialdone, A., and Srinivas, S. (2021).
1151 Single-cell transcriptomic characterization of a gastrulating human embryo. *Nature*, 600(7888),
1152 285-289.

1153 Tzertzinis, G., Ganatra, M. B., Ruse, C., Taron, C. H., Causey, B., Wang, L., and Schildkraut, I.
1154 (2023). The AMP deaminase of the mollusk *Helix pomatia* is an unexpected member of the
1155 adenosine deaminase-related growth factor (ADGF) family. *PloS One*, 18(7), e0286435.

1156 Van Haastert, P. J. (1983). Binding of cAMP and adenosine derivatives to *Dictyostelium*
1157 *discoideum* cells. Relationships of binding, chemotactic, and antagonistic activities. *Journal of*
1158 *Biological Chemistry*, 258(16), 9643-9648.

1159 Wakamiya, M., Blackburn, M. R., Jurecic, R., McArthur, M. J., Geske, R. S., Cartwright Jr, J.,
1160 and Kellems, R. E. (1995). Disruption of the adenosine deaminase gene causes hepatocellular
1161 impairment and perinatal lethality in mice. *Proceedings of the National Academy of Sciences*
1162 *(USA)*, 92(9), 3673-3677.

1163 Walsh, J., and Wright, B. E. (1978). Kinetics of net RNA degradation during development in
1164 *Dictyostelium discoideum*. *Microbiology*, 108(1), 57-62.

1165 Wang, B., and Kuspa, A. (2002). CulB, a putative ubiquitin ligase subunit, regulates prestalk cell
1166 differentiation and morphogenesis in *Dictyostelium* spp. *Eukaryotic Cell*, 1(1), 126-136.

1167 Wang, M., and Schaap, P. (1985). Correlations between tip dominance, prestalk/prespore pattern,
1168 and cAMP-relay efficiency in slugs of *Dictyostelium discoideum*. *Differentiation*, 30(1), 7-14.

1169 Wang, M., and Schaap, P. (1989). Ammonia depletion and DIF trigger stalk cell differentiation
1170 in intact *Dictyostelium discoideum* slugs. *Development*, 105(3), 569-574.

1171 Weijer, C. J. (2009). Collective cell migration in development. *Journal of Cell Science*, 122(18),
1172 3215-3223.

1173 White, G. J., and Sussman, M. (1961). Metabolism of major cell components during slime mold
1174 morphogenesis. *Biochimica et biophysica acta*, 53(2), 285-293.

1175 Wiechetek, M., Breves, G., and Höller, H. (1979). The effect of ammonium ion concentration on
1176 the activity of adenylate cyclase in various rat tissues in vitro. *Quarterly Journal of Experimental*
1177 *Physiology and Cognate Medical Sciences: Translation and Integration*, 64(3), 169-174.

1178 Williams, G. B., Elder, E. M., and Sussman, M. (1984). Modulation of the cAMP relay in
1179 *Dictyostelium discoideum* by ammonia and other metabolites: possible morphogenetic
1180 consequences. *Developmental Biology*, 105(2), 377-388.

1181 Williams, J. G. (1988). The role of diffusible molecules in regulating the cellular differentiation
1182 of *Dictyostelium discoideum*. *Development*, 103(1), 1-16.

1183 Williams, J. G. (2006). Transcriptional regulation of *Dictyostelium* pattern formation. *EMBO*
1184 *Reports*, 7(7), 694-698.

1185 Williams, J. G., Duffy, K. T., Lane, D. P., McRobbie, S. J., Harwood, A. J., Traynor, D., Kay, R.
1186 R. and Jermyn, K. A. (1989). Origins of the prestalk-prespore pattern in *Dictyostelium*
1187 development. *Cell*. 59(6), 1157–1163.

1188 Xu, J., Wang, X., Chen, J., Chen, S., and Li, Z., Liu, H., Bai, Y and Zhi, F. (2020). Embryonic
1189 stem cell-derived mesenchymal stem cells promote colon epithelial integrity and regeneration by
1190 elevating circulating IGF-1 in colitis mice. *Theranostics,* 10(26), 12204.

1191 Yamada, T. (1950). Dorsalization of the ventral marginal zone of the *Triturus* gastrula. I.
1192 Ammonia-treatment of the medio-ventral marginal zone. *The Biological bulletin*, 98(2), 98-121.

1193 Yeung, S. M. H., Shoshani, I., Stübner, D., and Johnson, R. A. (1989). Ammonium ions enhance
1194 proteolytic activation of adenylate cyclase and decrease its sensitivity to inhibition by "P"-site
1195 agonists. *Archives of Biochemistry and Biophysics*, 271(2), 332-345.

1196 Yoshino, R., Morio, T., Yamada, Y., Kuwayama, H., Sameshima, M., Tanaka, Y., Sesaki, H.,
1197 and Iijima, M. (2007). Regulation of ammonia homeostasis by the ammonium transporter AmtA
1198 in *Dictyostelium discoideum*. *Eukaryotic Cell*, 6(12), 2419-2428.

1199 Zavialov, A. V., Yu, X., Spillmann, D., Lauvau, G., and Zavialov, A. V. (2010). Structural basis
1200 for the growth factor activity of human adenosine deaminase ADA2. *Journal of Biological*
1201 *Chemistry*, 285(16), 12367-12377.

1202 Zhou, Q et al. (2014). Early-onset stroke and vasculopathy associated with mutations in
1203 ADA2. *New England Journal of Medicine*, 370(10), 911-920.

1204 Zurovec, M., Dolezal, T., Gazi, M., Pavlova, E., and Bryant, P. J. (2002). Adenosine deaminase-
1205 related growth factors stimulate cell proliferation in *Drosophila* by depleting extracellular
1206 adenosine. *Proceedings of the National Academy of Sciences (USA)* 99(7), 4403-4408.

1207

Figure 1

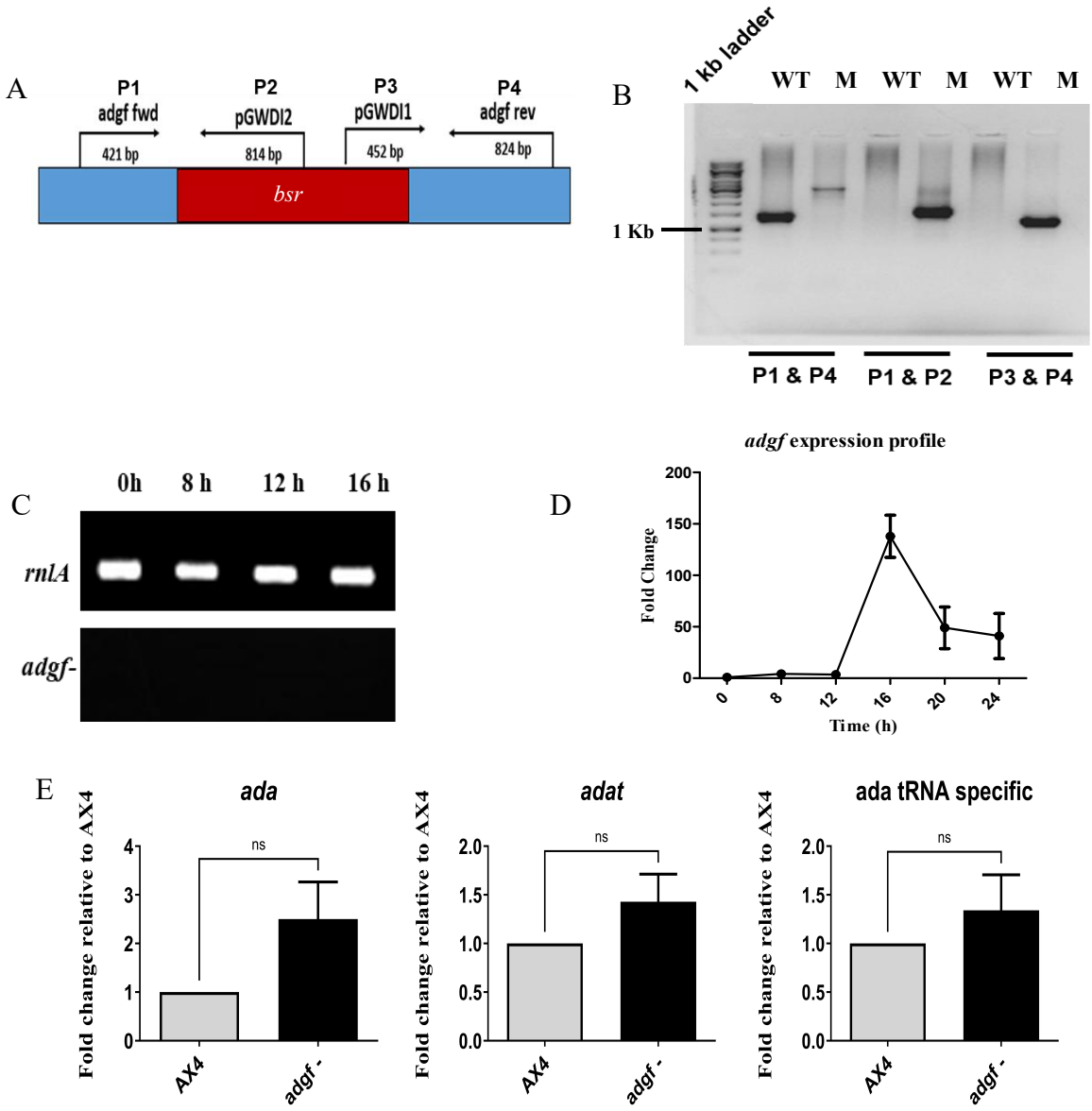

Figure 1. Mutant validation

A) Blasticidin resistance cassette (*bsr*) insertion in the *adgf* gene. **B)** PCR analyses using P1 and P4 primers. 1.4 kb shift in the *adgf* mutant. PCR using P1 and P2 primers showed an amplicon from the mutant (M) and not from the wild type (WT). PCR using P3 and P4 primers showed an amplicon with adgf mutant while WT did not show any amplicon. **C)** Semi-quantitative RT-PCR of internal control, *rnlA* and *adgf* $^{-}$. *adgf* expression during development in *Dictyostelium*. **D)** Total RNA was isolated from *Dictyostelium* during vegetative growth and development using TRIzol method. To quantify *adgf* expression, qRT-PCR was carried out with *rnlA* as a control and the fold change was calculated accordingly. Time points are shown in hours (bottom). Error bars represent the mean and SEM (n = 3). **E)** RT-PCR analysis was performed to check the expression of the isoforms of ADA during 16 h in the mutant.

Figure 2

A

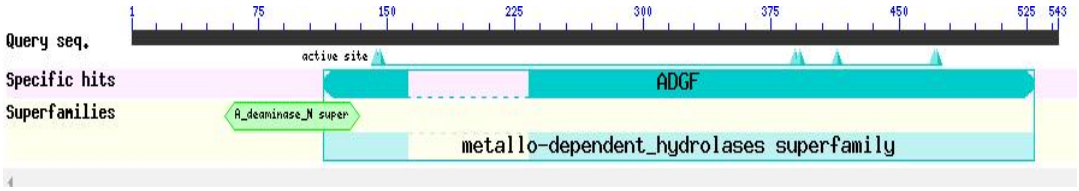

B

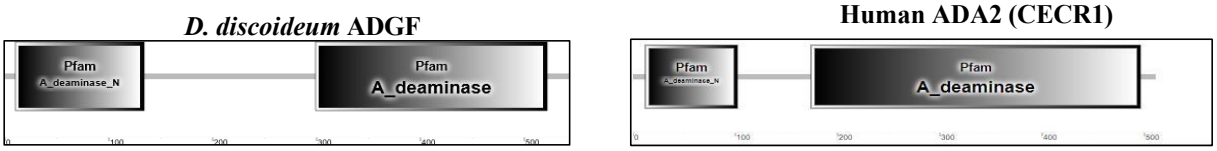

C

```
Q553U5     ADA2_DICDI        1   MFLK-------FKNIFFIVLTLSIVFNGLIVNSKNIHINNKNNNNNNNNKDLSSSESGSS    53
A0A3Q2UK74 A0A3Q2UK74_CHICK  1   --MK----PPSGQGIRLACL-LGLASLCL-------------------------------   22
A0A3Q1NIS4 A0A3Q1NIS4_BOVIN  1   -----MSGRLAPPSLLLALV-VSSFCPAT-------------------------------   23
Q9NZK5     ADA2_HUMAN        1   MLVDGPSERPALCFLLLAVA-MSFFGSAL-------------------------------   28
G3QXR5     G3QXR5_GORGO      1   MLVDGPSERPALRFLLLAVA-MSFFGSAL-------------------------------   28
A0A287BDN3 A0A287BDN3_PIG    1   -----MSGWPVLPALLLAVA-MSSFHSAT-------------------------------   23
Q1X7G4     Q1X7G4_XENLA      1   ----------MTCISHWLLL-LSLASAAL-------------------------------   18
F6NKG5     F6NKG5_DANRE      1   --MSSISLKD-VSAAVMVVL-LVCVSECK-------------------------------   25
Q9VVK5     Q9VVK5_DROME      1   -------MSPVIRRNLIACL-TLGLCVCLSFGPGPVE--SRTRPKNQVDRKLL-TIYGST    49
```

D

```
Q553U5     ADA2_DICDI        394  ILYN---NTNLYDAILLNTKRIGHGIQLPKHPLLMDLVLKNDIGIEICPISNQILQYVSD   450
A0A3Q2UK74 A0A3Q2UK74_CHICK  359  DWQGTSVDNNVLDALLLNTSRIGHGLALTKHPVAKNLSLKRDIPVEVCPISNQVLLVSD   418
A0A3Q1NIS4 A0A3Q1NIS4_BOVIN  360  DWEGTSVDRNILDAVILNSTRIGHGFALSKHPAVLAEAWKKDIPIEVCPISNQVLKLVSD   419
Q9NZK5     ADA2_HUMAN        361  DWQGTSIDRNILDALMLNTTRIGHGFALSKHPAVRTYSWKKDIPIEVCPISNQVLKLVSD   420
G3QXR5     G3QXR5_GORGO      361  DWQGTSIDRNILDALMLNTTRIGHGFALSKHPAVRTYSWKKDIPIEVCPISNQVLKLVSD   420
A0A287BDN3 A0A287BDN3_PIG    356  DWQGTSADRNILDALILNSTRIGHGFALSKHPAVWADAWRKDIPLEVCPISNQVLKLVSD   415
Q1X7G4     Q1X7G4_XENLA      355  TWQGKDVDENVLDALLLNTTRIGHGYALVKHPVARNLSLELNVPLEICPISNQVLLVSD   414
F6NKG5     F6NKG5_DANRE      353  DLDGTDVDRNVLDALLFNTSRIGHGFALVHHPVAKQLSRSRRVAVELCPISNQVLKLVSD   412
Q9VVK5     Q9VVK5_DROME      391  NWFGSTVDENLIDAILLGTKRIGHGFGLVKHPVVLDMLKKLNVAIEVNPISNQVLQLVSD   450
                                     .  : *: **:::::.*****  : :**         : :*: *****:*  ***
```

E

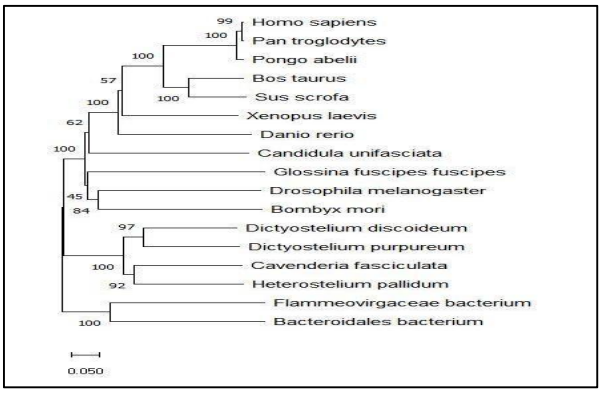

ADA2 (CECR1) *Homo sapiens* ADGF *D. discoideum* Overlap

F

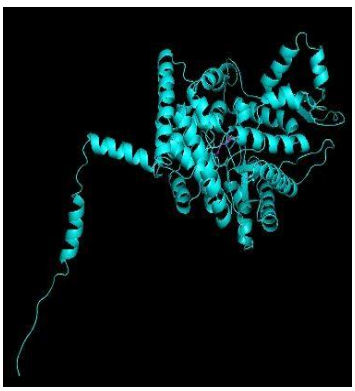

G

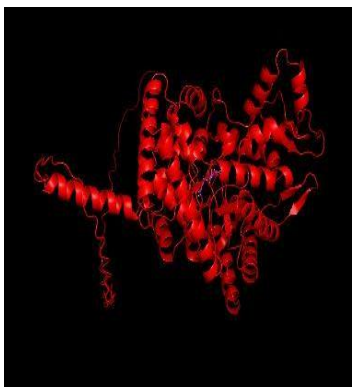

H

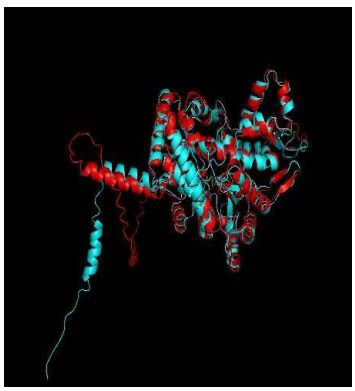

Figure 2. Bioinformatic analyses of ADGF

A) BLAST analysis of ADGF. ADGF belongs to the metallo dependent hydrolases superfamily. **B)** SMART analysis of different ADA domains within ADGF. ADGF protein has an adenosine deaminase-ADA domain and a N-terminal deaminase domain which is similar to the human ADA2. **Multiple sequence alignment of *Dictyostelium* ADGF with ADGF from other organisms. C)** The shaded region depicts the N-terminal signal sequence characteristic of extracellular proteins. **D)** The active site residue is highlighted in red. Active site residue is conserved between *D.discoideum* and human *ada2*. **E)** Phylogenetic analysis of ADGF across different organisms. Maximum likelihood method was used for constructing the tree using MEGAX (Molecular Evolutionary Genetic Analysis X). **Structural Comparison of human ADA2 and *Dictyostelium* ADGF.** Identical tertiary structures of human ADA2 and *Dictyostelium* ADGF. **F)** ADA2 (CECR1) *Homo sapiens* and **G)** ADGF *Dictyostelium discoideum* have many structural similarities. **H)** Alignment of *Dictyostelium* ADGF with Human ADA2 (CECR1).

Figure 3

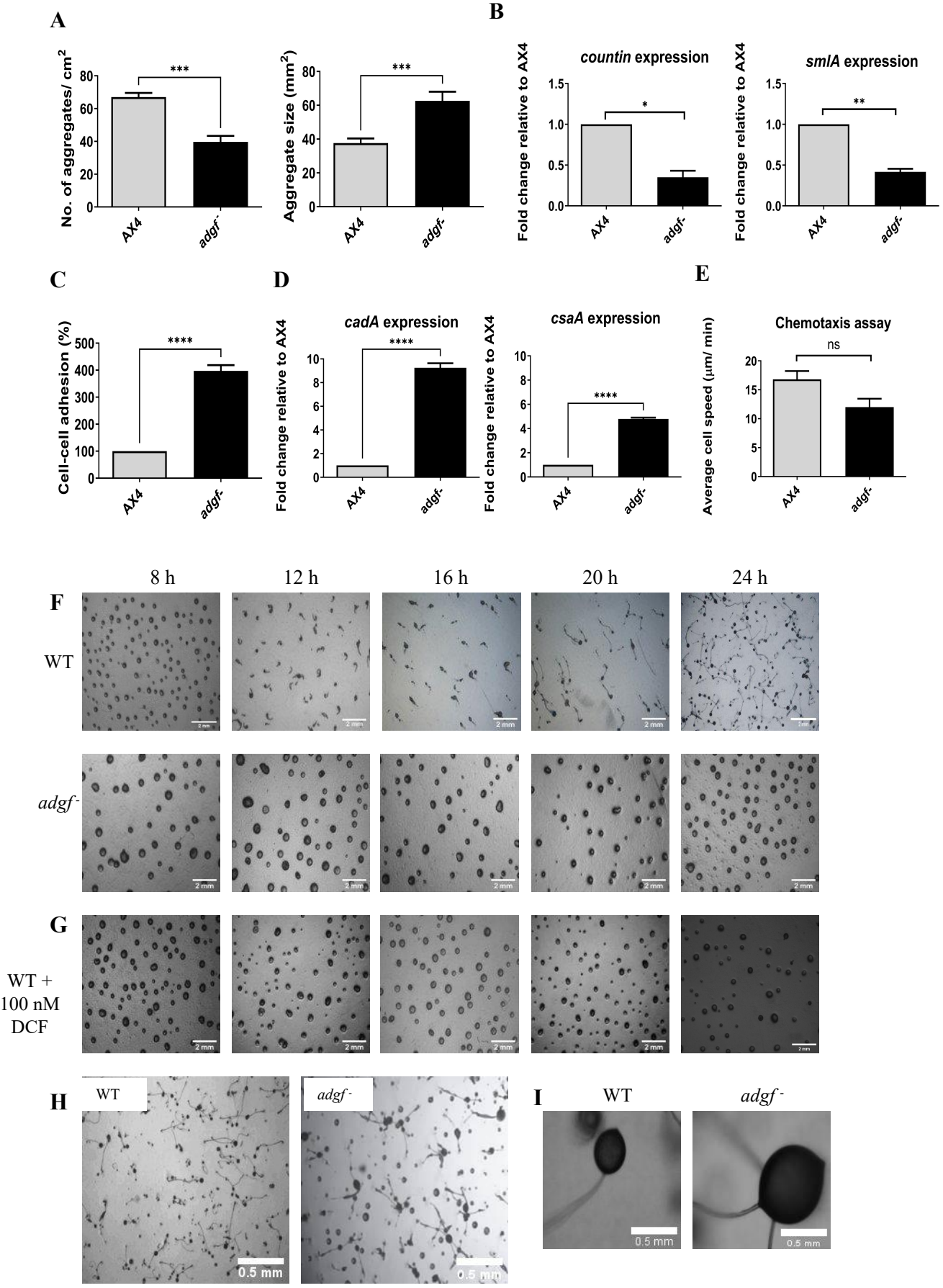
A
No. of aggregates/ cm2
***
AX4
adgf-
Aggregate size (mm2)
***
B
countin expression
Fold change relative to AX4
*
smlA expression
**
C
Cell-cell adhesion (%)
****
D
cadA expression
****
csaA expression
****
E
Chemotaxis assay
Average cell speed (µm/ min)
ns
8 h
12 h
16 h
20 h
24 h
F
WT
adgf-
G
WT + 100 nM DCF
H
WT
adgf-
0.5 mm
I
WT
adgf-
0.5 mm

Figure 3. Aggregates formed by *adgf*⁻ mutants are larger in size

A) The graph shows the number of aggregates formed by WT and *adgf*⁻ and their respective mound size. The values represent mean ± S.E; n=3. Significance level is indicated as *p< 0.05, **p< 0.01, ***p< 0.001, ****p< 0.0001. (Student's t-test). **B)** Expression levels of genes countin (*ctn*) and small aggregates (*smlA*) during aggregation in *adgf*⁻ compared to WT. *rnlA* was used as the internal control in the realtime PCR. **C)** WT and *adgf*⁻ cells were developed on KK2 agar, and after 16 h, the multicellular mounds/slugs were dissociated by vigorous vortexing in KK2 buffer. Individual cells were counted using a hemocytometer and resuspended in a phosphate buffer. Non-adherent single cells were counted 45 min after incubation. The percent cell-cell adhesion was plotted by normalizing the values to the non-adherent WT count to 100%. Error bars represent the mean ± SEM (n=3). Cell-cell adhesion, but not cAMP chemotaxis, is significantly impaired in *adgf*⁻. **D)** qRT-PCR analysis of cadherin (*cadA*) and contact site (*csA*) during aggregation. The fold-change in RNA transcript levels is relative to WT at the indicated time points. *rnlA* was used as the internal control (n=3). ns = not significant. **E)** Under agarose chemotaxis assay: The average cell speed in response to 10 µM cAMP was recorded. The graph represents the mean ± SEM (n=3). **Developmental phenotype of *adgf*⁻. F)** WT and *adgf*⁻ cells were washed, plated on 1% KK2 agar plates at a density of $5x10^5$ cells/cm^2, incubated in a dark, moist chamber and images were taken at different time intervals. **G)** WT cells treated with 100 nM of DCF mimicked the mound arrest phenotype of the mutant. The time points are indicated in hours at the top of the figure. Scale bar: 2 mm; (n=3). **H)** WT and *adgf*⁻ cells after 36 h of development. Scale bar: 0.5 mm; (n=3). **I)** Fruiting bodies of WT and *adgf*⁻. Scale bar: 0.5 mm; (n=3).

Figure 4

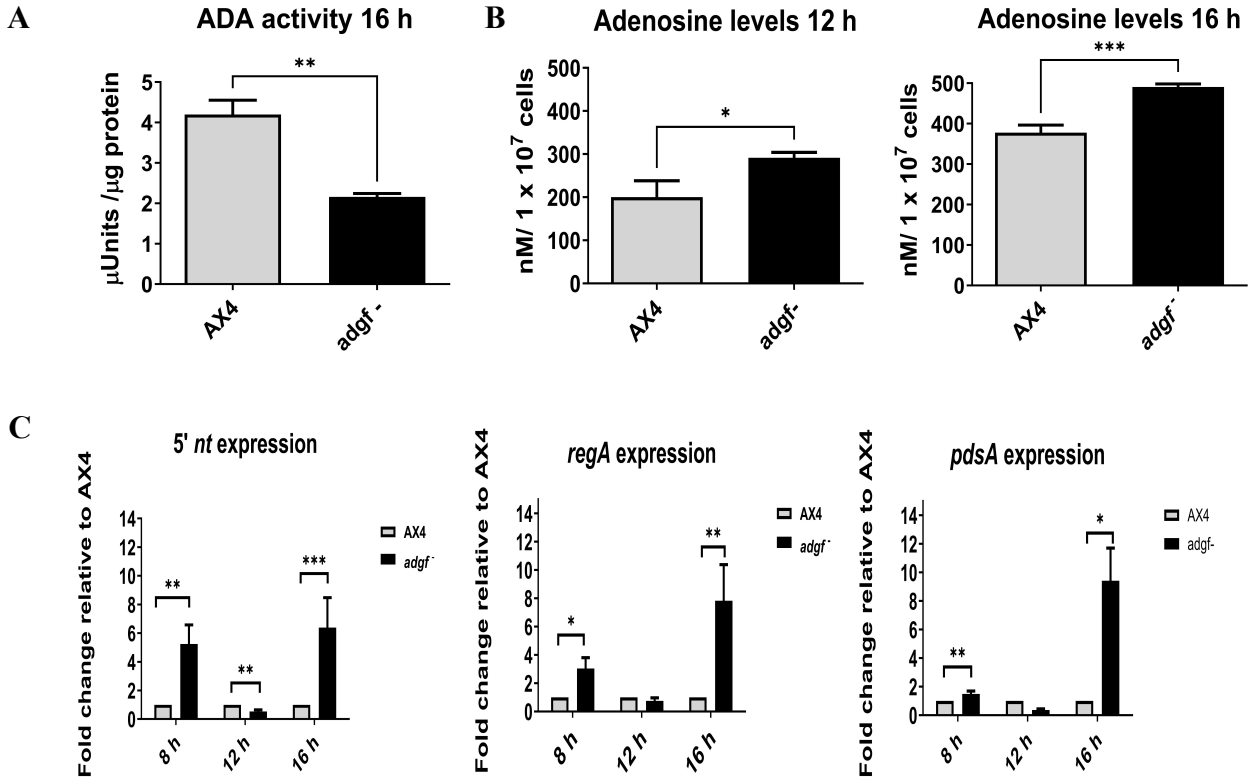

Figure 4. Reduced ADA activity and high adenosine levels in *adgf* $^{-}$

A) ADA activity in *Dictyostelium* cell extracts harvested at 16 h. The enzymatic assay for ADA was performed in *adgf* $^{-}$ with the corresponding WT control. Error bars represent the mean and SEM (n=3). Significance level is indicated as *p< 0.05, **p< 0. 01. Adenosine quantification and expression profile of genes involved in adenosine formation. **B)** Quantification of adenosine levels. Level of significance is indicated as *p< 0.05, **p< 0.01, ***p< 0.001; (n=3). **C)** Expression profile of the genes, 5' nucleotidase (5'*nt*) and phosphodiesterases (*regA*, *pdsA*) involved in cAMP-to-adenosine conversion. The fold-change in RNA transcript levels is relative to WT at the indicated time points. *rnlA* was used as an internal control. Error bars represent the mean and SEM (n=3).

Figure 5

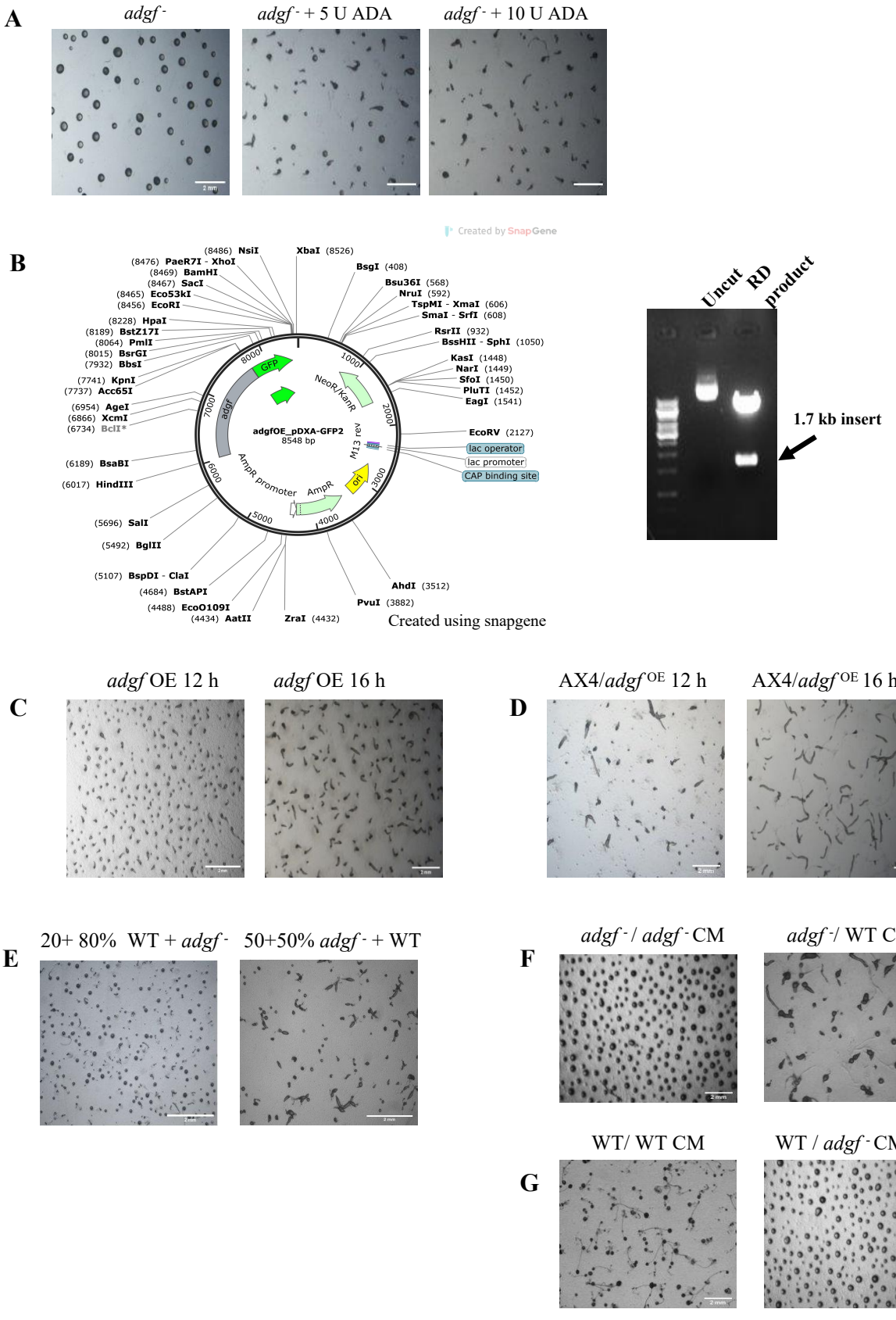
A
adgf -
adgf - + 5 U ADA
adgf - + 10 U ADA
B
Created by SnapGene
(8486) NsiI
XbaI (8526)
(8476) PaeR7I - XhoI
(8469) BamHI
(8467) SacI
(8465) Eco53kI
(8456) EcoRI
(8228) HpaI
(8189) BstZ17I
(8064) PmlI
(8015) BsrGI
(7932) BbsI
(7741) KpnI
(7737) Acc65I
(6954) AgeI
(6866) XcmI
(6734) BclI*
(6189) BsaBI
(6017) HindIII
(5696) SalI
(5492) BglII
(5107) BspDI - ClaI
(4684) BstAPI
(4488) EcoO109I
(4434) AatII
ZraI (4432)
AhdI (3512)
PvuI (3882)
BsgI (408)
Bsu36I (568)
NruI (592)
TspMI - XmaI (606)
SmaI - SrfI (608)
RsrII (932)
BssHII - SphI (1050)
KasI (1448)
NarI (1449)
SfoI (1450)
PluTI (1452)
EagI (1541)
EcoRV (2127)
lac operator
lac promoter
CAP binding site
adgfOE_pDXA-GFP2
8548 bp
GFP
NeoR/KanR
M13 rev
ori
AmpR
AmpR promoter
adgf
1000
2000
3000
4000
5000
6000
7000
8000
Created using snapgene
Uncut
RD product
1.7 kb insert
C
adgf OE 12 h
adgf OE 16 h
D
AX4/adgf OE 12 h
AX4/adgf OE 16 h
E
20+ 80% WT + adgf -
50+50% adgf - + WT
F
adgf - / adgf - CM
adgf -/ WT CM
G
WT/ WT CM
WT / adgf - CM

Figure 5. Overexpression of *adgf* rescued the mound arrest phenotype

A) *adgf* $^{-}$ mounds were treated with 5 U and 10 U ADA enzyme, plated for development and imaged at 16 h. Scale bar: 2 mm; (n=3). **B)** The full-length *adgf* gene was cloned in the vector pDXA-GFP2. The overexpression construct was verified by restriction digestion with HindIII and Kpn1 enzymes.**C)** Overexpression of *adgf* in the mutant rescued the mound arrest. **D)** Overexpression of *adgf* in the WT background. Scale bar: 2 mm; (n=3). The time points in hours are shown at the top. **WT cells reconstituted with *adgf* $^{-}$ rescued the *adgf* mutant phenotype. E)** Reconstitution of WT with *adgf* $^{-}$ in a 1:4 ratio showing a partial rescue and a full rescue of the *adgf* $^{-}$ mound arrest phenotype in a 1:1 ratio with WT. **F)** Development of *adgf* mutants in the presence of *adgf* $^{-}$ CM and WT CM on KK2 agar plates. WT CM rescued the mound arrest. **G)** Development of WT in the presence of WT CM and *adgf* $^{-}$ CM on KK2 agar plates. *adgf* $^{-}$ CM induced mound arrest in WT cells. Scale bar: 2 mm; (n=3).

Figure 6

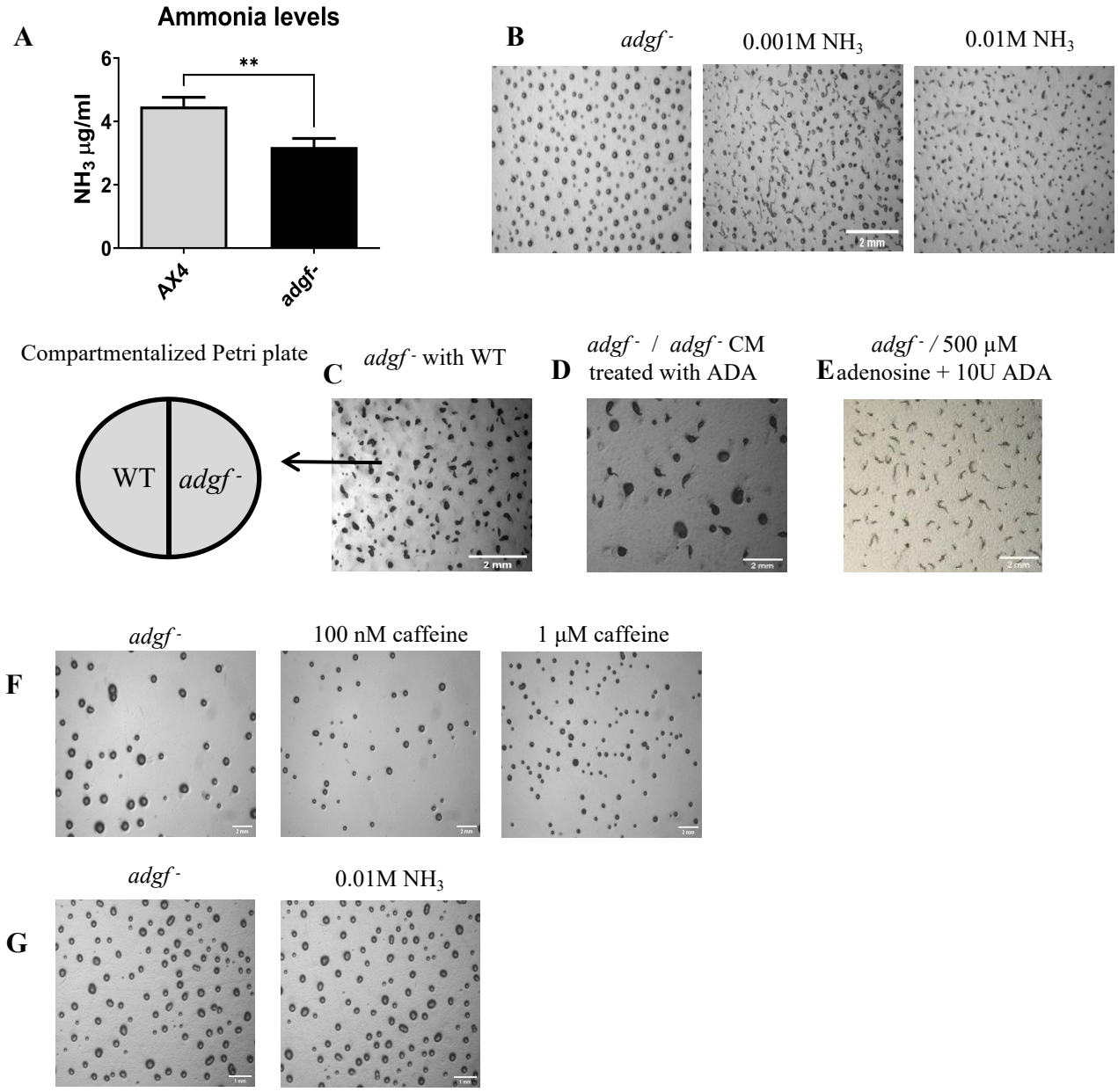
A
Ammonia levels
**
NH3 µg/ml
6
4
2
0
AX4
adgf-
B
adgf-
0.001M NH3
0.01M NH3
2 mm
Compartmentalized Petri plate
WT
adgf-
C
adgf- with WT
2 mm
D
adgf- / adgf- CM treated with ADA
2 mm
E
adgf- / 500 µM adenosine + 10U ADA
2 mm
F
adgf-
100 nM caffeine
1 µM caffeine
G
adgf-
0.01M NH3

Figure 6. Adenosine deamination reaction rescues the mound arrest of *adgf*⁻

A) Quantification of ammonia using the ammonia assay kit. WT and *adgf*⁻ mounds were harvested and lysed using a cell lysis buffer. Cell debris were removed by centrifugation, and the supernatant was used to quantify ammonia. **B)** Exposing *adgf*⁻ mounds to ammonia. Ammonia was generated by mixing 2 ml of NH_4Cl and 2 ml of 1N NaOH. The mixture was poured on top of the lid and the KK2 plates with the mounds were inverted and sealed thereafter. Images were taken 3.5 h post treatment. Dose dependent effect of ammonia on the rescue. Scale bar: 2 mm; (n=3). **C)** WT and *adgf*⁻ cells on either side of a compartmentalized Petri dish. **D)** *adgf*⁻ cells on one side of the plate in the presence of *adgf*⁻ CM treated with ADA enzyme in the other half of the dish. **E)** *adgf*⁻ cells on one side and KK2 buffer containing adenosine and ADA on the other half of the compartmentalized dish, rescued the mound defect. **Caffeine rescues the large mound size of *adgf* mutant**. **F)** *adgf*⁻ cells were treated with different concentrations of caffeine (100 nM, 1 µM) while plating and images were taken 3.5 h post chemical treatment. Scale bar: 2 mm; n=3. **G)** Exposure to ammonia does not rescue the aggregate size of *adgf* mutant. *adgf* - mounds were exposed to 0.01 M ammonia and images were taken 3.5 h post chemical treatment. Scale bar: 2 mm; (n=3).

Figure 7

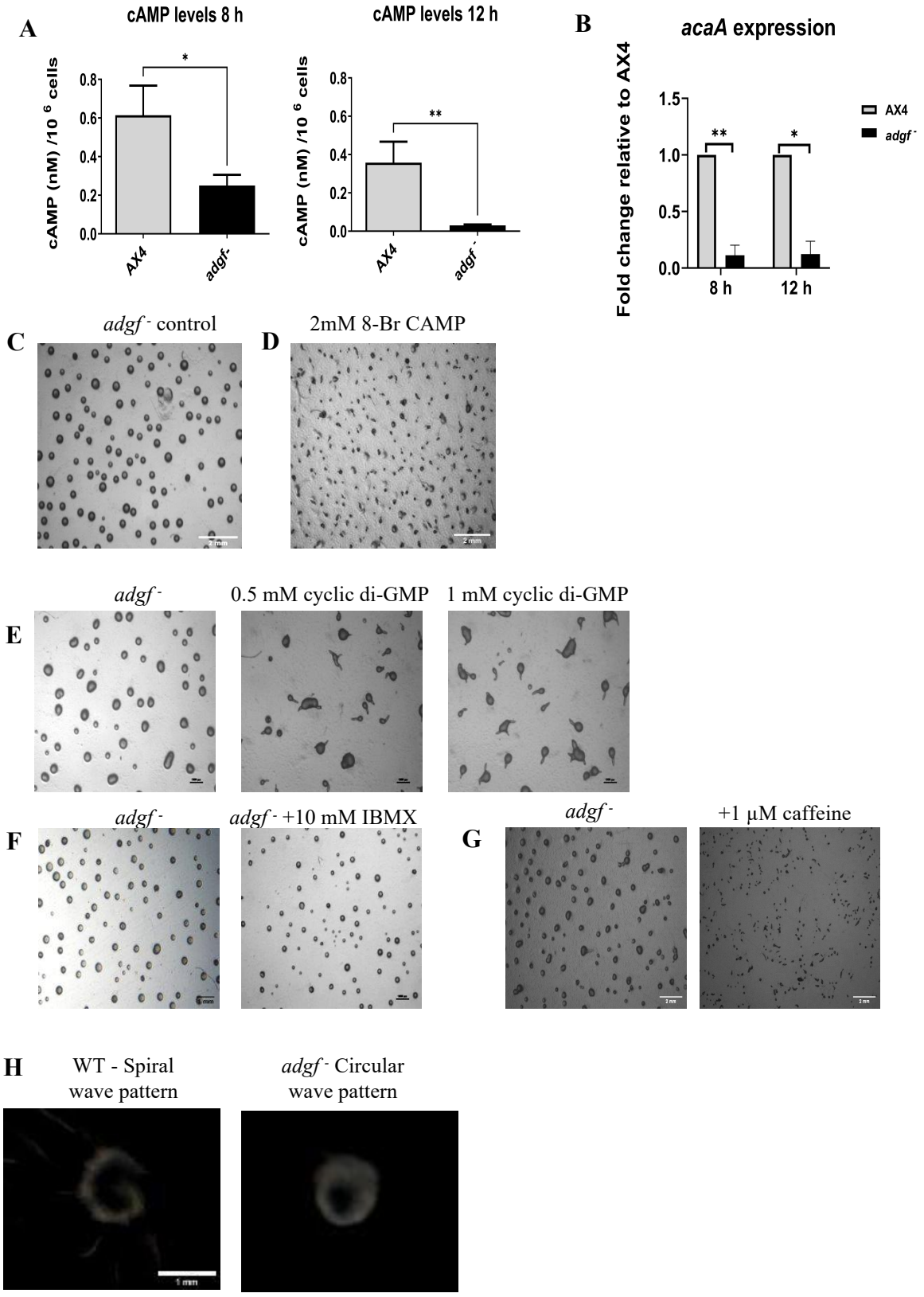
A
cAMP levels 8 h
cAMP levels 12 h
cAMP (nM) /10 6 cells
0.8
0.6
0.4
0.2
0.0
*
**
AX4
adgf-
B
acaA expression
Fold change relative to AX4
1.5
1.0
0.5
0.0
**
*
8 h
12 h
AX4
adgf-
C
adgf- control
D
2mM 8-Br CAMP
E
adgf-
0.5 mM cyclic di-GMP
1 mM cyclic di-GMP
F
adgf-
adgf- +10 mM IBMX
G
adgf-
+1 µM caffeine
H
WT - Spiral wave pattern
adgf- Circular wave pattern
1 mm

Figure 7. Impaired cAMP signaling in *adgf*$^-$

A) Total cAMP levels in WT and *adgf*$^-$ mounds were quantified using cAMP-XP assay kit (Cell signaling, USA). Level of significance is indicated as *p< 0.05, **p< 0.01; (n=3). **B)** *acaA* expression was quantified using qRT-PCR. The error bars represent the mean ± SEM (n=3). **C)** *adgf*$^-$ mounds. **D)** *adgf*$^-$ mounds were treated with 2 mM pkA activator 8-Br-cAMP and imaged after 3.5 h. Scale bar: 2 mm; (n=3). **Treatment with cyclic di-GMP and caffeine rescues the mound arrest phenotype. E)** Addition of cyclic-di-GMP restored tip formation in *adgf*$^-$ 4 h after the treatment. Scale bar: 1 mm; (n=3). **F)** PDE inhibitor (IBMX) treatment failed to rescue the *adgf*$^-$ mound arrest. Scale bar 1 mm; (n=3). **G)** *adgf*$^-$ mounds treated with caffeine formed tips 3.5 h post treatment. Scale bar: 2 mm; (n=3). **Altered cAMP wave pattern in *adgf*$^-$. H)** Optical density wave images depicting cAMP wave generating centers in WT and *adgf*$^-$. WT shows spiral wave pattern and *adgf*$^-$ exhibits circular wave propagation.

Figure 8

A

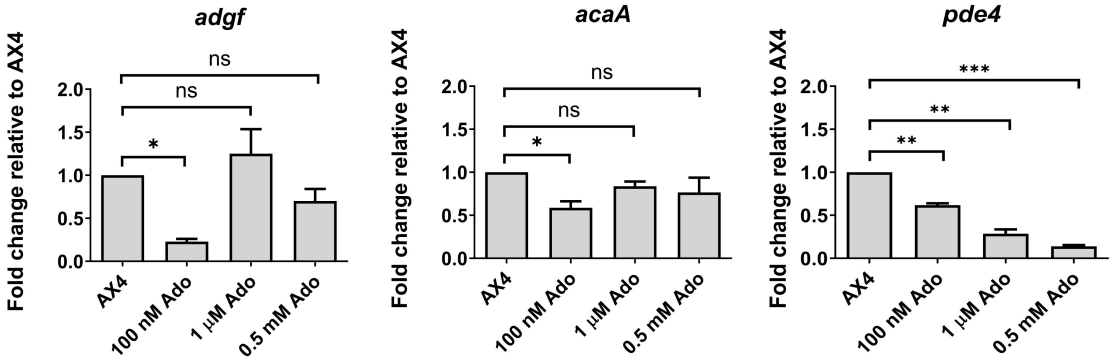
adgf
acaA
pde4
Fold change relative to AX4
ns
*
**
***
AX4
100 nM Ado
1 μM Ado
0.5 mM Ado

B

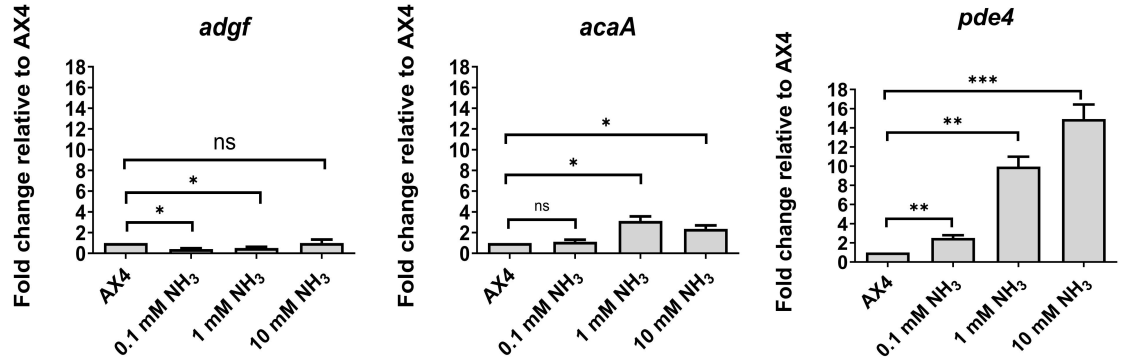
adgf
acaA
pde4
Fold change relative to AX4
ns
*
**
***
AX4
0.1 mM NH3
1 mM NH3
10 mM NH3

C

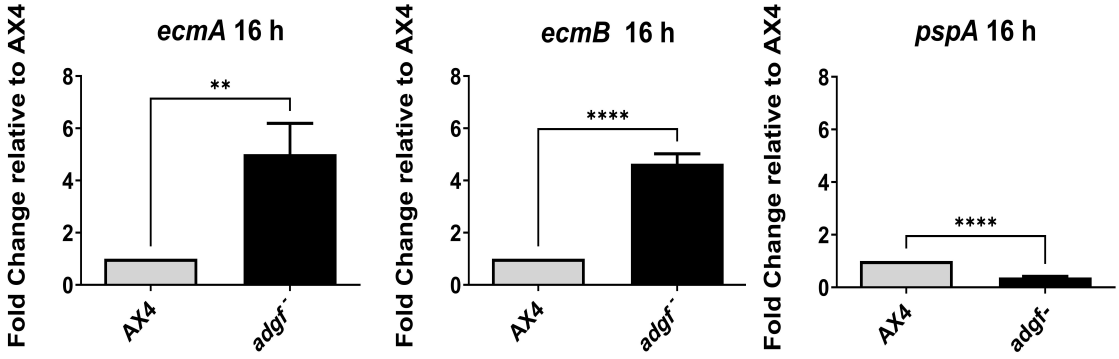
ecmA 16 h
ecmB 16 h
pspA 16 h
Fold Change relative to AX4
**
****
AX4
adgf-

Fig 8. Expression levels of *adgf*, *acaA* and *pde4* in response to adenosine and ammonia treatment

A) Expression levels of *adgf, acaA* and *pde4* in response to adenosine treatment (100 nM, 500 nM, 1 μM). **B)** Effect of different concentrations of ammonia (0.1 mM, 1 mM, 10 mM) on the expression levels of *adgf*, *acaA* and *pde4*. Levels of significance is indicated as *p<0.05, **p<0.01, and ***p<0.001; (n=3). **Expression levels of prestalk, *ecmA*, *ecmB* and prespore, *pspA* cell type markers in *adgf*$^{-}$.** The expression profiles of **C)** prestalk (*ecmA*, *ecmB*) and prespore (*pspA*) specific markers in WT and *adgf*$^{-}$ were quantified using qRT-PCR. Level of significance is indicated as *p<0.05, **p<0.01, ***p<0.001 and ****p<0.0001; (n=3). Three independent biological replicates were performed and the error bars represent the mean and SEM. The fold-change in RNA transcript levels is relative to WT at the indicated time points. *rnlA* was used as the internal control (n=3). ns = not significant

Figure 9

A

100% *adgf*$^{-}$ DIL

20% *adgf*$^{-}$ DIL – 80% AX4

B

100% AX4- DIL

20% AX4 DIL – 80% *adgf*$^{-}$

C

30% AX4/*adgf*^{OE} DIL – 70% *adgf*$^{-}$

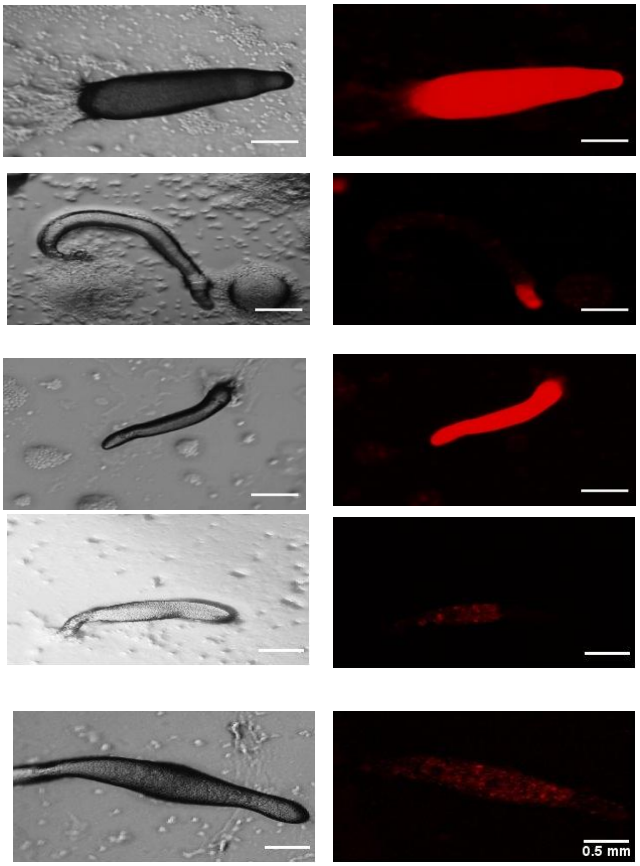

D

8 h

16 h

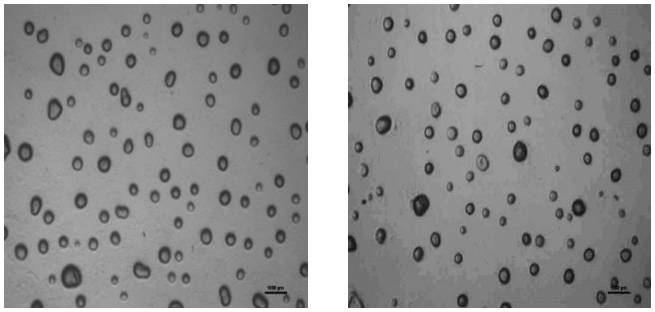

E

5 U ADA

10 U ADA

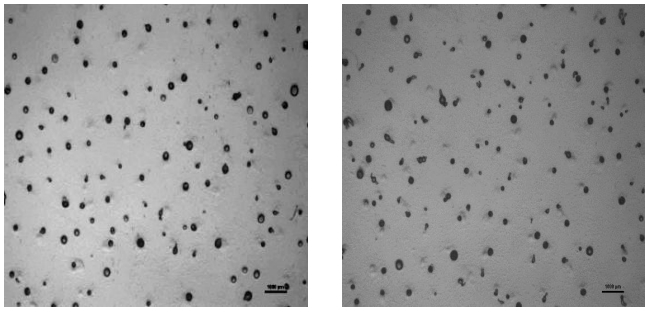

F

20 U ADA

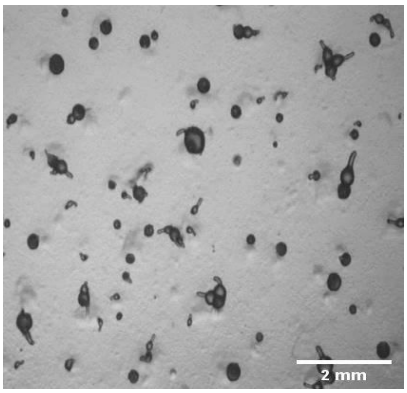

Figure 9. Reconstitution of WT cells with *adgf*$^{-}$ following DIL staining

A-C) DIL labelled cells were reconstituted with unlabeled cells and plated for development. Images were captured during the migrating slug stage. The left panel shows bright field, and the right panel shows the corresponding fluorescence images. Scale bar: 0.5 mm; (n=3). ***adgf* acts downstream of histidine kinase *dhkD*. D)** *dhkD*$^{-}$mutants on KK2 agar plates. **E-F)** 5 U, 10 U or 20 U ADA was added on top of the mounds. Scale bar: 1 mm; (n=3). Images were taken 3.5 h post treatment. Addition of the ADA enzyme rescued the mound arrest phenotype in a dose dependent manner. Scale bar: 2 mm; (n=3).

Figure 10

Model of *adgf* function

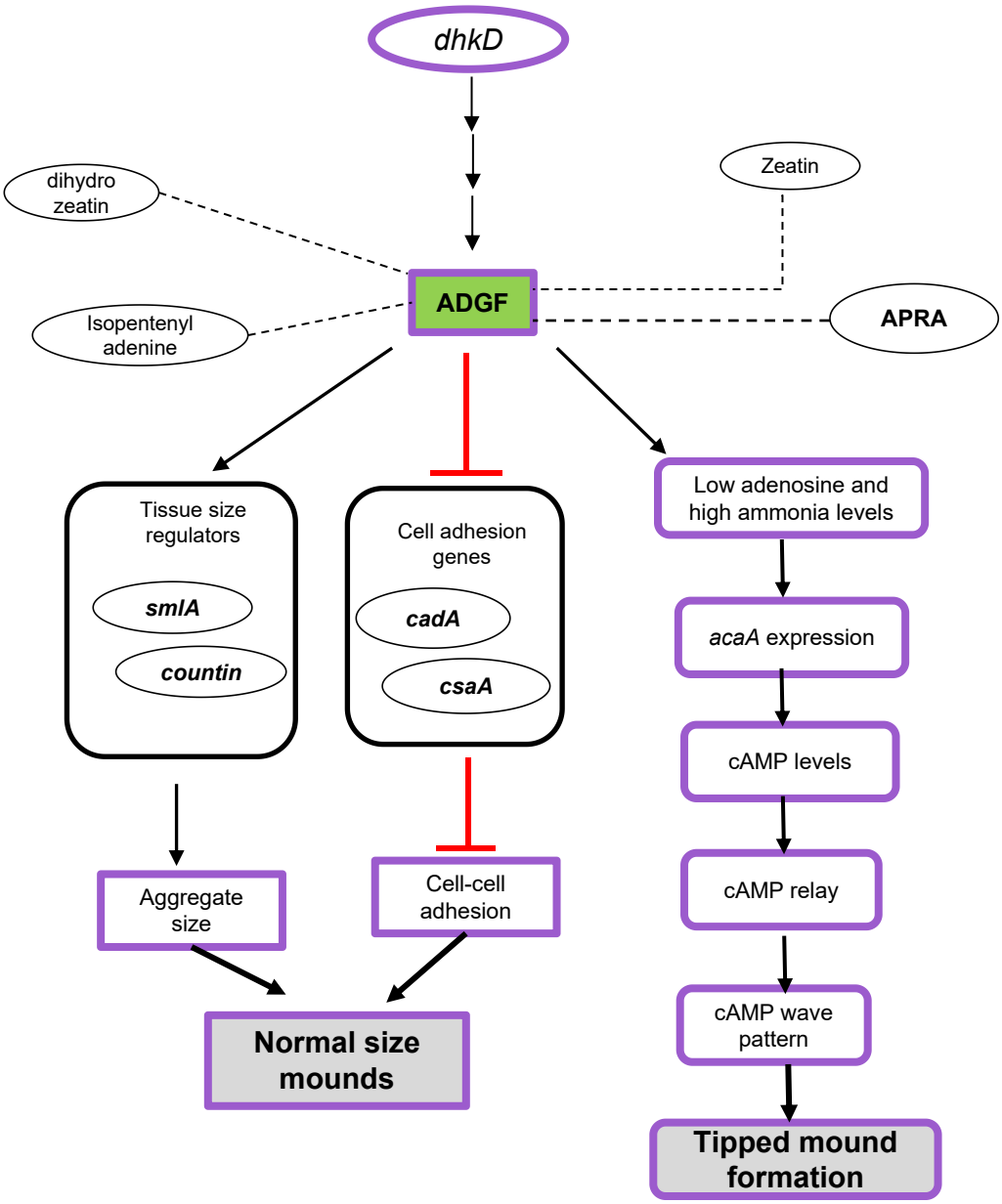

Fig 10. Model illustrating the role of *adgf* in development

adgf supresses the expression of genes involved in cell adhesion, *cadA and csaA*. *adgf* regulates aggregate size and tip development by directly acting on adenosine, ammonia levels and cAMP signaling. Line ending in an arrow implies that the previous gene/factor either directly or indirectly raises the activity or levels of the second; line ending in a cross-bar indicates inhibition. Dotted lines indicate ADGF interacting with APRA, and the cytokinins zeatin, dihydro zeatin and isopentenyl adenine.